2015

Gene expression noise in stress response as a survival strategy in fluctuating environments

Javier Garcia-Bernardo
University of Vermont

GENE EXPRESSION NOISE IN STRESS RESPONSE AS A SURVIVAL STRATEGY IN FLUCTUATING ENVIRONMENTS

A Thesis Presented

by

Javier Garcia-Bernardo

to

The Faculty of the Graduate College

of

The University of Vermont

In Partial Fullfillment of the Requirements
for the Degree of Master of Science
Specializing in Computer Science

May, 2015

Defense Date: March 27, 2015

Thesis Examination Committee:
Mary J. Dunlop, Ph.D., Advisor
Matthew J. Wargo, Ph.D., Chairperson
Margaret J. Eppstein, Ph.D.
Peter S. Dodds, Ph.D.
Cynthia J. Forehand, Ph.D., Dean of the Graduate College

Abstract

Populations of cells live in uncertain environments, where they encounter large variations in nutrients, oxygen and toxic compounds. In the fluctuating environment, cells can sense their surroundings and express proteins to protect themselves against harmful substances. However, if the stressor appears infrequently or abruptly, sensing can be too costly or too slow, and cells cannot rely solely on it. To hedge against the sudden appearance of a stressor, cell populations can also rely on phenotypic diversification through bet-hedging. In bet-hedging, cells exploit noise in gene expression or use multistable genetic networks to produce an heterogeneous distribution of resistance-conferring protein levels. In this thesis, we analyze novel roles of noise in biological systems. Through a combination of modeling and stochastic simulations, we find that noise can coordinate multi-component stress response mechanisms in a subset of the population with no extra cost. In addition, we use evolutionary algorithms to analyze the conditions where the benefits provided by noise in gene expression are equivalent to those of a more complicated, bistable distribution of protein levels. Our results show that for cells living in noisy fluctuating environments, both noise in gene expression and bistability show similar growth rates, meaning that noise in gene expression can be an effective bet-hedging strategy.

CITATIONS

Material from this thesis has been published in the following form:

Garcia-Bernardo J., Dunlop M.J.. (2015). Noise and Low-Level Dynamics Can Coordinate Multicomponent Bet Hedging Mechanisms. *Biophys. J.*.

AND

Material from this thesis is in submission in the following form:

Garcia-Bernardo J., Dunlop M.J.. Phenotypic diversity using bimodal and unimodal expression of stress response proteins in fluctuating environments. *In submission*.

Acknowledgements

First, I'd like to thank Dr. Mary Dunlop for the past three years. Her support, patience and expertise were fundamental in my academic development. Thanks for being always so helpful and motivational, for using an advising style that allowed me to be productive, explore many interesting areas, and do cool things like go to conferences. Thanks to the rest of my thesis committee: Dr. Maggie Eppstein, Dr. Matt Wargo and Dr. Peter Dodds, for their useful insights and time spent on my thesis. I'm also grateful to the rest of the research lab for creating a constructive and fun environment, especially to Nick Rossi for correcting my English all the time.

Gracias también a mi familia, por darme la oportunidad de estar aquí. A mis amigos, a los que dejé en Europa y los nuevos, porque ellos son la diferencia entre un master y pasar unos de los mejores años de mi vida.

Table of Contents

List of Figures

List of Tables

Chapter 1

Introduction

> *"Everything may evaporate at any instant. Everything!" I said with surprising vehemence. "You, me, the most rocklike personality since Calvin Coolidge; death, destruction, despair may strike. To live your life assuming otherwise is insanity."*
>
> — Luke Rhinehart, *The Dice Man*.

Through our history, human beings have been surrounded by microorganisms. Microbial infections have killed millions of people, with relatively high mortality rates until the discovery of antibiotics and vaccination– although increasing antibiotic resistance may change this (1). However, microorganisms have also been the base of many beneficial products, such as vinegar, cheese, bread and beer for more than 6000 years (2). Today, we have expanded the positive role that microbes play in our lives to include medical and industrial products, including aminoacids, vitamins, antibiotics, probiotics, biocontrol agents, pesticides, enzymes, biofuels and many others (2). From the point of view

of the microorganism, the environment is always changing, with stressors appearing suddenly. For example, bacteria get exposed to antibiotics as the result of its use in medicine and livestock. Similarly, the fungi *Penicillium* and lactic acid bacteria, used in the cheese industry, face continuous changes in temperature and sugar availability (3, 4). Understanding the mechanisms that microorganims use to survive in uncertain environments has applications in both medicine and industry.

In an environment where many toxins are present, microbes have mechanisms to protect themselves against general stresses. For example, they express pumps to export toxins, block pores to stop the influx of the stressor, and produce reductases to detoxify the environment (5). In addition, many bacteria can enter growth arrest or sporulate to avoid damage (6–8). However, these general mechanisms are very taxing for the cells (9). Microorganisms use two main strategies to balance growth in basal, un-stressed conditions, with high survival rates in the presence of a stressor. First, cells can sense and adapt to the environment. Nevertheless, the population of cells faces complete annihilation if action of the stressor is faster than the time required to adapt to it. In addition, sensory mechanisms have also an associated cost, which can be larger than the damage of the stressor if this is only encountered rarely. Thus, cells cannot rely solely on sensory mechanisms if the stressor appears suddenly or infrequently. A second strategy consists on diversifying the isogenic population to hedge against future stresses, where part of the population is in charge of growing in the absence of stress and part of the population produces the costly stress resistance mechanisms (10). To allow for variability within one single genotype, switching between phenotypic states may be driven by noise, although it can be coupled with sensing mechanisms (10). Population diversification is a common strategy *in vivo*. In *Saccharomyces cerevisiae*, many stress response genes contain a TATA-box in their

promoter region, which has been shown to increase gene expression variability and protect against the appearance of future stresses (11). Similarly, variability in *Escherichia coli* has also been associated with stress survival (7).

Networks with interlinked fast positive and slow negative feedbacks are often associated with variability in gene expression (12). One of such networks, the *multiple antibiotic resistance* (*mar*) operon, is an important stress response mechanism in *E. coli* (13). The *mar* operon is composed of three genes. The activator, MarA, is translated rapidly and induces the operon, as well as more than 40 genes implicated in general stress response (13, 14). The repressor and sensor MarR, is translated slowly and represses the operon (14). MarR is inactivated by many toxic compounds, allowing for the production of MarA and the initialization of the response (13). The third gene, *marB*, has recently been found to be an indirect repressor of the operon (15). In a previous study by Garcia-Bernardo and Dunlop (16), we developed a stochastic model of the *mar* operon. We showed that the combination of slow negative and fast positive feedbacks can produce stochastic pulses in the expression of MarA when no stressor is present, increasing resistance to the sudden appearance of a stressor. Moreover, our computational model shows the response is tunable, and variability is decreased when MarA is induced (via MarR repression), ensuring low variability and a large, reliable response in the presence of a stressor. We further showed that the parameter regime of the system balances low cost to the cell, since resistance mechanisms are expressed in pulses, and elevated resistant to antibiotics via phenotypic variability. Finally, we accounted for the cost of expressing stress response mechanisms and the benefit of surviving the sudden appearance of a stressor to calculate the growth rate in fluctuating environments. Our results showed that variability can increase the fitness of the population in a a fluctuating environment, but not in a fixed one.

In our previous study, the resistance to the stressor was calculated directly from the level of MarA. Therefore, we showed that noise can increase the survivable concentration of a stressor when the resistance is controlled by one gene. Similar results have been observed *in vivo*. For example, yeast strains with increased heterogeneity in the expression of *Ura3p*, a gene that converts *5-fluoroorotic acid* into a toxic compound, survive higher concentrations of the acid (17). However, general stress resistance is often composed of many complementary genes regulated by one or a few regulators (18). Even when noise can be transmitted (19), transmission only occurs infrequently, and it is not clear if noise or low-level fluctuations in the level of the regulator can coordinate multi-component resistance mechanisms. To test this, we used a stochastic model to simulate the transmission of noise and dynamics from a regulator to its downstream genes (Section 2.1, (20)). We compared several upstream regulator dynamics, including constant expression, low-level pulsatile dynamics and noisy expression. We found that both low-level pulses and noisy expression are able to coordinate expression of multiple downstream genes in a small fraction of the population. For example, the low-level pulsatile dynamics of MarA in unstressed conditions are able to coordinate its 40 downstream genes. Moreover, this coordination increases the survival concentration of a stressor without an increase in energy expenditure in the population. Therefore, noise may increase growth rates in fluctuating environments both when the resistance mechanism is composed of one gene and when it is composed of many genes controlled by an upstream regulator.

When noise is used to diversify the population, the distribution of protein levels in the population is usually unimodal. Another survival strategy in fluctuating environments consists of diversifying the population into a finite number of phenotypes (10). In this case, the distribution of resistance levels in the population is multimodal. Several examples of

multimodal systems have been found *in vivo*. In many pathogenic bacteria, such as the ones causing tuberculosis, *Mycobacterium tuberculosis*, or staph infections, *Staphylococcus aureus*; a small portion of the population remains in a non-growing, resistant state called persistance (6, 21). Since many stressors are only effective when cells are metabolically active, this population can survive sudden fluctuations in the concentration of a stressor. Other pathogenic bacteria, such as the agents causing pneumonia, *Streptococcus pneumoniae*, or gonorrhea, *Neisseria gonorrhoeae*, enter competence under nutrient limitation. Competence is a state of cell growth arrest where cells have the ability to uptake extracellular DNA (22). Some others, such as the microbes causing botulism, tetanus and colitis, from the genre *Clostridum*, are able to form spores during starvation, which are non-growing cells that are highly resistant cells to stresses (22). In addition, several mathematical analyses have been shown the benefit of bimodality in systems with two environmental states and two phenotypes (23–28). Finally, bacteria such as *E. coli*, *Lactococcus lactis* and *S. aureus* that grow in a mix of primary carbon-sources (such a glucose) and secondary carbon-sources (such as lactose, arabinose or cellobiose) express genes to uptake the secondary sugars in a small fraction of the population. In bacteria, the strigent response is activated if the primary sugar is depleted before the cells are able to adapt to the secondary sugar, resulting in growth arrest until a primary sugar becomes available (29). Producing the transporters in a subset of the popultion allows the population to continue growing even if the primary carbon-source never becomes available (29).

However, the apparent benefits of multistability contrast with the fact that the expression of more than 99% of *E. coli* genes is well described by gamma distributions of protein (30), as the expected fothe result of noisy gene expression (31). To bring insight into the conditions where multistability is benefitial, we created a model of a population of cells growing in

an environment that fluctuates between low and high stress conditions. We represented the population by the distribution of concentrations of a protein conferring stress resistance. Growth rate was determined by the cost of expressing the resistance protein in the absence of stress and the benefit of expressing the machinery in the presence of a stress. We then used evolutionary algorithms to find optimal or near-optimal distributions of proteins in fluctuating environments, where growth rate was the measure of fitness driving the evolution process. To allow for a comparison between unimodal (modeling noise in gene expression) and bimodal distributions, we restricted the evolved distribution to be a gamma distribution (unimodal) or the weighted sum of two gamma distributions (bimodal). We systematically varied the time spent in the presence of low and high concentrations of a strong stressor, i.e. a compound that kills the cells that do not express enough stress response protein. In these conditions, bimodality was favoured when the population spends large times in low stress, and unimodal distributions adapted to high stress conditions were evolved otherwise. We further allowed the cells to sense and adapt to the environment. Sensing populations can afford large cell loses the first time they encounter a stressor, since they then adapt to the stress and can regenerate. Consequently, we found that sensing increases the parameter region where bimodality is favoured. Importantly, for both sensing and no sensing cases, we found that the benefit of bimodality decreases as the noise or the number of environments is increased. Therefore, unimodal distributions can be optimal bet-hedging strategies under realistic fluctuating environments.

Through a combination of modeling, stochastic simulations and evolutionary algorithms, we find that noise in gene expression can be an effective bet-hedging strategy. When stress response depends on multiple genes, noise in an upstream regulator can coordinate the response in a small fraction of the population, increasing stress survival without an increase

in metabolic cost. Furthermore, when the stress level in the environment is variable, noise in downstream gene expression, which creates unimodal distribution of protein levels, provides the same benefit than a more complicated, bimodal strategy.

Chapter 2

Journal Papers

2.1 Noise and Low-Level Dynamics Can Coordinate Multicomponent Bet-Hedging Mechanisms

184 Biophysical Journal Volume 108 January 2015 184–193

Article

Noise and Low-Level Dynamics Can Coordinate Multicomponent Bet Hedging Mechanisms

Javier Garcia-Bernardo[1] and Mary J. Dunlop[2,*]
[1]Department of Computer Science and [2]School of Engineering, University of Vermont, Burlington, Vermont

ABSTRACT To counter future uncertainty, cells can stochastically express stress response mechanisms to diversify their population and hedge against stress. This approach allows a small subset of the population to survive without the prohibitive cost of constantly expressing resistance machinery at the population level. However, expression of multiple genes in concert is often needed to ensure survival, requiring coordination of infrequent events across many downstream targets. This raises the question of how cells orchestrate the timing of multiple rare events without adding cost. To investigate this, we used a stochastic model to study regulation of downstream target genes by a transcription factor. We compared several upstream regulator profiles, including constant expression, pulsatile dynamics, and noisy expression. We found that pulsatile dynamics and noise are sufficient to coordinate expression of multiple downstream genes. Notably, this is true even when fluctuations in the upstream regulator are far below the dissociation constants of the regulated genes, as with infrequently activated genes. As an example, we simulated the dynamics of the multiple antibiotic resistance activator (MarA) and 40 diverse downstream genes it regulates, determining that low-level dynamics in MarA are sufficient to coordinate expression of resistance mechanisms. We also demonstrated that noise can play a similar coordinating role. Importantly, we found that these benefits are present without a corresponding increase in the population-level cost. Therefore, our model suggests that low-level dynamics or noise in a transcription factor can coordinate expression of multiple stress response mechanisms by engaging them simultaneously without adding to the overall cost.

INTRODUCTION

Cells can use stochastic gene expression (noise) and dynamics to diversify isogenic populations to hedge against stress (1). For example, in bacterial persistence, a small fraction of cells stochastically enters a dormant, drug-resistant state, allowing the population to insure against the sudden appearance of an antibiotic (2,3). An excitable gene circuit in *Bacillus subtilis* drives the temporary transition to competence under nutrient limitation (4,5). These are infrequent events: <1% of *Pseudomonas aeruginosa*, *Staphylococcus aureus*, and *Escherichia coli* cells are in the persistence state, and 3% of *B. subtilis* cells initiate competence under nutrient limitation (4–6). However, stress response mechanisms often require expression of many genes simultaneously, and single regulators may control many downstream targets. These observations raise the question of how multiple rare events are coordinated. A key principle of bet hedging is that the cost to the overall population is low, because only a small subset of cells initiates a response. We extended this idea by asking whether coordinated expression of downstream genes could further mitigate overall cost.

Single-cell resolution measurements have revealed that cellular processes involved in stress response and environmental change have high levels of phenotypic variability. For example, systematic noise measurements across the *Saccharomyces cerevisiae* proteome have demonstrated that noise levels are high for proteins involved in stress response, amino acid synthesis, and heat shock (7). TATA-box-containing genes associated with stress response in *S. cerevisiae* exhibit fluctuations that protect against future environmental changes (8). Variability can come from noise sources that are intrinsic or extrinsic, where intrinsic noise is unique to individual genes and variability is produced by random events in transcription, translation, and degradation. Extrinsic noise is produced by variability in processes that affect many genes in the same way; for instance, differences in growth or numbers of ribosomes in a cell can produce correlated expression of many genes (9–12). Diversity can also be driven by dynamic changes in gene expression as a result of the regulatory architecture. For instance, regulatory proteins can exhibit repetitive pulses in expression even in the absence of external inputs that drive this behavior (13,14). Examples of pulsing include the yeast regulator Msn2 under glucose, osmotic, and oxidative stress (15,16); Crz1 in response to calcium stress (17); and KatG in *Mycobacterium* to control persistence (18). Specific networks, such as coherent feed-forward loops, have been shown to increase population heterogeneity, enhancing drug resistance (19). Phenotypic diversity of stress-response mechanisms, derived from stochastic gene expression or other

Submitted August 12, 2014, and accepted for publication November 10, 2014.

*Correspondence: mjdunlop@uvm.edu

Editor: Reka Albert.

0006-3495/15/01/0184/10 $2.00

http://dx.doi.org/10.1016/j.bpj.2014.11.048

dynamics, plays an important role in protecting against future uncertainty.

Interestingly, many stress response mechanisms are members of single-input or multi-input modules, where one or a few regulatory proteins control the expression of many downstream genes (20). This regulatory motif is overrepresented in genetic networks that respond to exogenous conditions such as diauxic shift and DNA damage (21). In response to stress, Msn2 from *S. cerevisiae* regulates hundreds of target genes (15). Crz1 exhibits pulses that activate >40 genes (17). The alternative sigma factor σ^B in *B. subtilis* exhibits noise-driven pulses, regulating >100 genes (22). The multiple antibiotic resistance activator MarA in *E. coli* controls >40 downstream genes involved in resistance to antibiotics (23,24). Therefore, understanding how noise or dynamics in an upstream regulator influences expression of diverse downstream genes is of great interest in understanding stress response. An upstream regulator could potentially achieve the concentration necessary to activate the simultaneous expression of multiple downstream genes. However, achieving infrequent coordination in a small subset of the total population would require complex regulation or long-term memory. The alternative strategy presented here is to rely on low-level fluctuations in the activator to coordinate multiple rare events.

Whether a signal is propagated depends upon whether the downstream promoter can decode the variability in the transcription factor, as determined by the promoter and the properties of the signal (15,25–28). If the dynamics of the downstream promoter are fast, that is, the binding and unbinding rates are faster than degradation, cell division, and changes in the upstream input, then the output will follow the input (25). If they are slow, then most of the input dynamics will be filtered (16). For example, input pulses that are high in amplitude or duration will activate the promoter (16), but small pulses and noise that do not meet these requirements will rarely activate downstream promoters. Although activation is infrequent, the downstream genes will still be activated a small fraction of the time due to the stochastic nature of gene expression; these rare events produce long tails in the mRNA and protein distributions (29–31).

There is a cost associated with the expression of stress-response genes. In general, cells allocate their resources to optimize growth, but the expression of genes not immediately related to growth can provide a potential benefit if the environment changes. This cost-benefit relationship has been observed in vivo: for lactose intake, populations of *E. coli* are able to grow fastest in the presence of lactose if the *lac* operon is expressed moderately, but not if expression is high (32). For antibiotic resistance, cells are able to grow in higher concentrations of antibiotic if the *mar* operon is moderately induced (33,34). Therefore, there is a tradeoff between the burden imposed by the expression of these genes and the benefits they can provide in an uncertain environment.

To understand how noise and dynamics in a stress response regulator are propagated to downstream target genes, we performed stochastic simulations using three types of inputs: constant expression, pulsatile dynamics, and intrinsic/extrinsic noise. The regulators control the expression of several downstream genes, creating a single-input module similar to those observed in natural networks. We found that downstream genes regulated by all types of inputs have noisy expression profiles; however, fluctuating inputs (due to pulsatile dynamics or intrinsic/extrinsic noise) can coordinate the temporal pattern of downstream gene expression. This effect becomes pronounced when there are several downstream genes, because the probability of multiple genes being coordinated is higher when a dynamic input can orchestrate the response. The fidelity with which the input is propagated to the downstream genes depends upon the characteristics of the downstream promoter and the input signal. Notably, even low-level fluctuations in an upstream regulator can serve to hedge against stressors without adding to the overall cost. Coordination of downstream genes may allow cells to hedge against future uncertainty in the environment without an excessive burden to the population.

MATERIALS AND METHODS

Stochastic model

All downstream genes in all simulations are subject to intrinsic noise. To simulate this, we used a stochastic model based on the processes described below, for which the reaction rates are given in Table S1 in the Supporting Material and shown in Fig. S1. Exact stochastic simulations were conducted using the Gillespie algorithm (35).

Binding and unbinding of the regulator to the promoter of the downstream gene are modeled by

$$P + A \xrightarrow[\kappa_{ON}]{} P'$$

$$P' \xrightarrow[\kappa_{OFF}]{} P + A,$$

where P represents the promoter in the unbound state, A is a transcription factor, and P' is the promoter in the bound state.

Transcription and translation are modeled using

$$P \xrightarrow[\alpha]{} P + M$$

$$P' \xrightarrow[\alpha']{} P' + M$$

$$M \xrightarrow[\beta]{} M + D,$$

where M is the mRNA for the downstream gene and D is the protein encoded by the downstream gene. Presence of the transcription factor increases the transcription rate ($\alpha' > \alpha$). The translation rate, β, includes both translation and folding events.

mRNA and protein degradation are modeled by

$$M \xrightarrow[\lambda_M]{} \varnothing$$

$$D \xrightarrow[\lambda_D]{} \varnothing,$$

where the rates λ_M and λ_D model mRNA and protein degradation and dilution due to cell growth.

We considered constant and pulsing inputs for the transcription factor profiles. For the constant case, the activator level is set to 250 molecules for all time. To define the activator levels, the pulsing input case uses the function

$$A = \begin{cases} 500\left(1+\sin\left(\frac{t}{6\pi}-\frac{\pi}{2}\right)\right), & 0<t\leq 120 \\ 0, & 120<t<240 \end{cases}.$$

The signal is repeated every 240 min, creating periodic pulses of the regulator. The mean of the pulsing signal is 250 molecules, identical to the mean of the constant activator. We used an arbitrary periodic waveform represented by a sine wave followed by a period with no activator, so that signal properties including amplitude, pulse duration, and frequency could be adjusted explicitly.

Cross correlation

The cross correlation measures the correlation between two time series, $f(t)$ and $g(t)$, when a lag, τ, is applied to one of the two signals. We used the unbiased estimate of the cross correlation:

$$R_{f,g}(\tau) = \begin{cases} \frac{1}{N-|\tau|}\sum_{t=0}^{N-|\tau|-1} f(t+\tau)g(t), & \tau\geq 0 \\ R_{gf}(-\tau), & \tau<0 \end{cases}.$$

Here, $f(t)$ and $g(t)$ are the time series for the transcriptional regulator and a downstream protein. Both signals are mean subtracted and normalized by dividing by the standard deviation. N is the number of time points.

Amplitude response plots

For three different dissociation constant (K_D) values (100, 1000, and 10,000 molecules), we varied the amplitude of the pulses from 10^{-2} K_D to 10^2 K_D, and ran a simulation keeping all other parameters constant. The resulting time series for the protein levels of the activator and downstream genes were used to calculate the maximum cross correlation.

Cost functions

We developed functions describing the cost and benefit of expressing a downstream gene. The cost term has two parts: a term c_1 that quantifies the burden of expressing proteins that are not needed for growth under baseline, nonstressed conditions, and a second term, c_2, which quantifies how cells are impacted in an environment with a stressor present. The total cost is assumed to be Bliss-independent (36) and is given by

$$c(D,S) = c_1 + c_2 - c_1 \times c_2,$$

where the cost is a function of the downstream protein levels, D, and the stressor, S.

The burden of protein expression is modeled as in Dekel and Alon (32):

$$c_1(D) = \frac{n_0 D}{1-\frac{D}{M}},$$

where M is the maximal capacity for nonessential proteins, D is the concentration of the downstream protein, and n_0 is a normalization constant.

The impact of a stressor is modeled as in studies by Wood and Cluzel (33) and Greco et al. (37):

$$c_2\left(S_{\text{eff}}\right) = \frac{S_{\text{eff}}^n}{k^n + S_{\text{eff}}^n},$$

where S_{eff} is the effective concentration of the stressor, k is the half-inhibition constant, and n is the Hill coefficient.

Following the formulation from Wood and Cluzel (33), the benefit is measured as a decrease in c_2. By decreasing the intracellular concentration of toxic compound, the relation between the extracellular concentration of the stressor, S, and the effective concentration, S_{eff}, is

$$S_{\text{eff}} = \frac{S}{1+B},$$

where B is the benefit of expressing the stress response machinery, given by

$$B(D) = \frac{b_{\max} D}{k_b + D}.$$

Here, $b_{\max}$ is the maximum benefit of expressing the machinery and k_b is the concentration of protein that gives the half-maximal response.

We used the following parameter values in the cost and benefit equations: $M = 15{,}000$ molecules, $n_0 = 1\times10^{-5}$, $k = 1$ mM, $n = 2$, $b_{\max} = 10$, and $k_b = 15{,}000$ molecules. M and n_0 were set such that $c_1(D)$ falls between 0 and 1. k sets the maximum concentration of stressor that the cells can survive when no resistance mechanisms are expressed, and n determines the steepness of $c_2(S_{\text{eff}})$, whereas $b_{\max}$ and k_b together set the maximum concentration that cells can survive when the resistance mechanisms are present. The results are not specific to the values used. We also tested another cost function, which depends linearly on the levels of D, $c_1(D) = D/M$ (Fig. S2), and observed similar benefits with coordination.

Maximum survivable concentration of stressor and cost without stressor

To quantify the maximum concentration of stressor that a population of cells can survive, we calculated the cost for each cell with the stressor (recall that the benefit of expressing resistance genes reduces the cost) and determined which cells survived. To determine survival, we imposed an arbitrary threshold of 0.95. Cells that exceed this threshold are dead and those with costs below it survive. We increased the concentration of the stressor until only 0.1% of cells in a simulated population of 10^6 cells survived. We define the concentration at which this occurs as the maximum survivable concentration. Our findings are not sensitive to the exact threshold values selected.

We performed these calculations by simulating long time courses (10^7 min) to generate distributions of downstream protein levels. Using this distribution, we calculated the cost for each point in the distribution. We verified that distributions of downstream protein levels generated using this approach are equivalent to those generated by running many shorter simulations and extracting data associated with the final time point (see Supporting Materials and Methods and Fig. S3).

The cost of growing without a stressor was calculated as the average of the costs for each of 10^7 cells in the simulation.

Multiple antibiotic resistance operon in *E. coli*

We simulated expression of genes in the *mar* operon, as in Garcia-Bernardo and Dunlop (38), using the Gillespie algorithm to obtain values of MarA as a function of time. Experimental data is available for the K_D values of nine downstream genes (39). We simulated 40 downstream genes by including multiple instances of each of the known values. The specific K_D values, assuming a cell volume of 10^{-15} L, are 7,830 (4), 10,239 (4), 15,058 (8), 18,069 (20), and 24,092 (4) molecules, where the number of instances of each gene included is shown in parentheses.

Extrinsic and intrinsic noise in the activator

To model extrinsic noise, we allowed K_{ON} to vary with time (as in Shahrezaei et al. (40)) in the activator and downstream genes. We used an exact numerical solution of an Ornstein-Uhlenbeck process. Extrinsic noise was simulated using the method of Gillespie (41), with code from http://www.mathworks.se/matlabcentral/fileexchange/30184-exact-numerical-simulation-of-the-ornstein-uhlenbeck-process. The code generates a time series for a source of extrinsic noise $\varepsilon(t)$, with zero mean and standard deviation equal to

$$\sigma = \sqrt{c \times \frac{T}{2}}.$$

The relaxation time, T, was set to 40 min (42), and the diffusion constant, c, was set to 0.006 (low noise), 0.02 (medium noise), 0.05 (high noise), where the parameters used in Shahrezaei et al. (40) fall between our medium and high noise cases. Following methods of Shahrezaei et al. (40) and Fox et al. (43), we replaced the parameter K_{ON} with

$$K_{ON} \times \frac{e^{\epsilon(t)}}{\langle e^{\epsilon(t)} \rangle},$$

which generates a lognormal distribution, suitable to model fluctuations due to extrinsic noise (26,40,42).

We modeled intrinsic noise in the activator using the Gillespie algorithm (35). Reactions and rates are the same as those for the downstream genes given in Table S1, with the following modifications: $K_{OFF} = 0.1$ min^{-1}, $K_{ON} = 1$ (molecules min)$^{-1}$, $\alpha' = 1$ min^{-1}, $\lambda_M = 0.1$ min^{-1}, $\beta = 1$ min^{-1}, and $\lambda_D = 0.02$ min^{-1}.

Although mean activator expression is identical for the three noise levels, the mean of the downstream gene will depend upon the noise levels. To correct for this, we adjusted K_{ON} for the downstream genes, as indicated in Table S2.

Based on the method of Shahrezaei et al. (40), we handled time-dependent propensities, $a(t)$, in the Gillespie algorithm by approximating $\int_t^{t+\tau} a(t)dt$ with $a(t)\tau$. This approximating is valid when changes in $a(t)$ are slow compared with the reaction times (i.e., the difference between $a(t)$ and $a(t + \tau)$ is small), as is the case in this study.

Coordination of *n* downstream genes

To calculate the fraction of cells in a population with n downstream genes expressed in a coordinated fashion we ran simulations of n downstream genes for 10^7 minutes, each using the same activator profile as input. For each time point, we checked how many cells had all downstream genes coordinated simultaneously. To measure this, we set a threshold of 1000 molecules and counted the number of downstream genes that exceeded the threshold. The fraction of cells with coordination in n genes is determined by dividing the number of cells where all n downstream genes exceeded the threshold by the number of cells where this was not achieved. Our results are not sensitive to the exact threshold values selected.

RESULTS AND DISCUSSION

Input dynamics can coordinate rare events

To study how expression of multiple downstream genes is impacted by the dynamics of a single input, we developed a stochastic model in which the promoter of a downstream gene can be in one of two states (44–46). In the active promoter state, a transcriptional activator is bound, leading to elevated levels of transcription relative to the inactive state, where the activator is not bound. The model includes reactions for transcription, translation, and degradation of mRNA and proteins (Methods). Many transcriptional regulators are expressed at basal levels and activated in the presence of stress, such as heat, nutrient limitation, or other environmental factors. Under unstressed conditions, having a small subset of the population express these genes can act as an insurance policy against future uncertainty. Furthermore, transcription factors operate on diverse downstream genes with a range of dissociation constants (K_D). This includes transcription factors with K_D values well above the physiological levels of the activator (see examples in the literature (16,39,47,48)). This allows a single transcription factor to differentially activate each of its downstream target genes. Therefore, we focused on downstream target genes with promoters that have K_D values well above the mean of the input (Fig. 1). By doing this, we are looking at rare events, as would be expected in bet hedging.

Initially, we compared two alternative upstream regulator dynamics and their impact on the expression of downstream genes. In the first case, the activator is held constant. In the second case, we considered a transcription factor that exhibits pulsatile expression, with a pulse followed by a

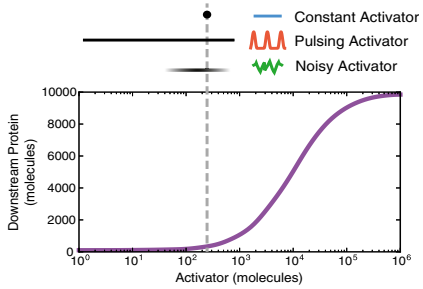

FIGURE 1 Input dynamics for a downstream gene. Activation curve for a downstream gene with a dissociation constant (K_D) of 10,000 molecules. The range of three activator dynamics is displayed above the figure: constant, pulsing, and intrinsic/extrinsic noise. In each case, the mean of the activator signal (*gray dashed line*) is identical. To see this figure in color, go online.

constant off state. We use the term pulsing here to describe time-varying signals, ranging from periodic oscillations to stochastic fluctuations in protein levels (13). For simplicity of analysis, we initially used a periodic input signal with uniform pulses followed by periods of low activator levels (Materials and Methods). However, as discussed later, our results do not require that the expression of the transcription factor be periodic or the pulse sizes uniform. We set the mean expression of the two transcription factors (constant and pulsing) to be identical to allow for a controlled comparison between the two types of input dynamics.

Even with a constant input, intrinsic noise due to stochastic events causes noise in expression of downstream genes (Fig. 2 *A*). Similar dynamics were observed in the pulsing case, but the transcription events are associated with the input pulse (Fig. 2 *B*). Because the fluctuations in the input are low compared with the K_D of the downstream gene, the transcription factor only intermittently turns on downstream gene expression and most variation is due to intrinsic noise. Although not every pulse in the input initiates expression of the output, when transcription is initiated, it is coordinated with the input pulse. When averaged over many downstream genes, fluctuations from the constant-input case average out, whereas fluctuations from the pulsed-input case follow the input (Fig. 2, *A* and *B*). Importantly, the distributions of downstream proteins are very similar for constant and pulsing inputs and have similar tails (Fig. 2 *C*), indicating that the frequency with which the downstream genes are in an elevated state of expression is similar for genes under both types of control. These results suggest that it is important to consider the timing of when genes are expressed and not just static expression data.

We next asked how propagation of input dynamics depends on the dissociation constant of the promoter for the downstream gene. We calculated cross correlations between the input signal and the downstream proteins. The cross correlation measures the similarity of two signals as a function of time (Materials and Methods). Because expression of the downstream gene follows the input pulse, there is a lag in the cross correlation, with the maximum cross correlation indicating how well the two signals are correlated after the signal is transmitted. As expected given the lack of input dynamics, there is no correlation between the input and downstream protein levels in the constant case, regardless of K_D (Fig. 2 *D*). In contrast, the pulsing input produces correlations between the input signal and the downstream protein. The highest correlations are from cases where the K_D is near or below the mean of the input, as expected, since it is easy to activate expression of downstream genes whose promoter has high affinity for the activator. As the K_D increases, the correlation goes down. Notably, the correlation persists for K_D values two orders of magnitude above the mean of the activator. Therefore, even infrequent activation events show correlation with the input signals, despite being far from the dynamic range of the downstream gene. This result is important because it suggests that even genes that appear

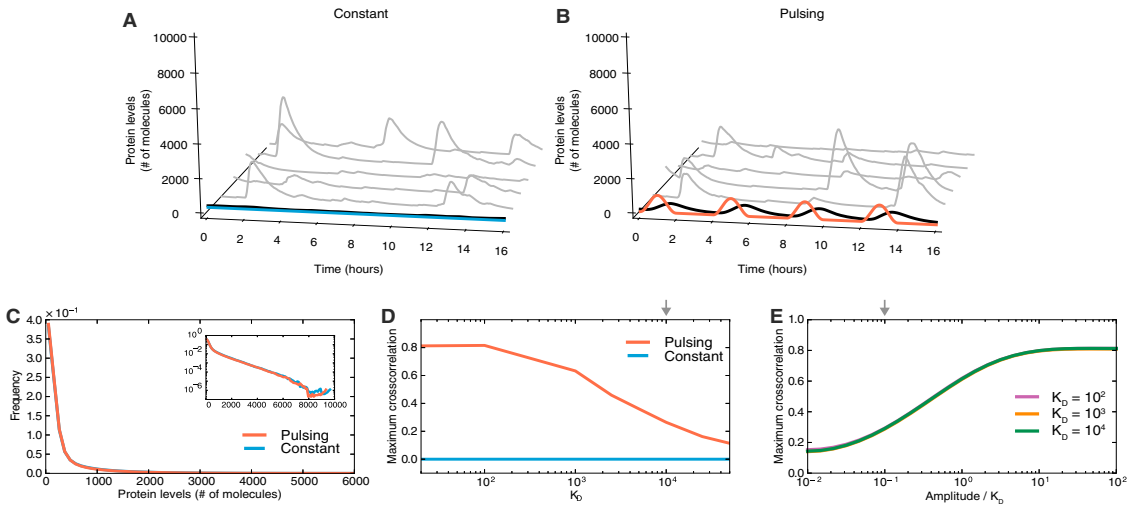

FIGURE 2 Pulsing-coordinates expression of downstream genes. (*A* and *B*) Downstream gene expression given a constant (*blue*) or pulsing (*red*) input. Protein levels for five representative downstream genes (*gray*) are shown, along with the mean of 1000 genes (*black*). (*C*) Histograms of downstream protein expression for constant and pulsing activator dynamics. (*Inset*) Same data as in the main figure, but on a semilogarithmic scale. (*D*) Maximum cross correlation between the activator signal and downstream protein as a function of K_D. The K_D used in the simulations shown in *A–C* is marked with an arrow. (*E*) Maximum cross correlation between a pulsing activator and three downstream genes with different dissociation constants as a function of the amplitude to the K_D ratio. The ratio used in the simulations in *A–C* is indicated with an arrow. To see this figure in color, go online.

not to be activated in population studies may be initiated rarely but in a coordinated fashion, providing an organized response, as might be necessary for bet hedging.

We also asked what impact the amplitude of the pulsing input has on the maximum cross correlation. When normalized by the K_D, the maximum cross-correlation curves are equivalent for all amplitudes (Fig. 2 *E*). Therefore, the important quantity is the ratio of the pulse amplitude to the K_D, with fluctuations well below the K_D still resulting in measurable levels of correlation between input and output signals. These results are consistent with those of previous studies showing that pulses in gene expression can be propagated: in Msn2 in yeast (15), NF-κB in mice (49,50), and the stress sigma factor σ^B in *B. subtilis* (22), pulses in the input are highly correlated with pulses in their respective downstream genes.

To test the generality of our results, we examined a system with fast promoter binding dynamics. In this case, transcription-factor binding and unbinding at the promoter is rapid, such that expression of the downstream gene is initiated more frequently, but the duration of each burst of expression is shorter (Supporting Materials and Methods). Again, we observed correlation between the pulsed input and the downstream output for K_D values well above the mean of the pulsed input (Fig. S4 *A*). We also asked whether our results were resistant to the inclusion of explicit cellular growth and partitioning and found that those processes have only minor contributions to the correlation observed between activator and downstream gene, as well as between two downstream genes (Supporting Materials and Methods and Fig. S5).

Coordination is achieved without added cost

We next asked what role the correlation between pulses in the input and initiation of expression of the downstream genes had on the regulation of multiple genes. As a model for a single input module, we simulated expression of 10 downstream genes, all regulated by a single transcription factor. We conducted numerical experiments with increasing concentrations of stressor, quantifying the maximum concentration of stressor that a population can survive (Materials and Methods). In addition, we calculated the population-level cost of expressing stress resistance genes using a cost function that we derived from previously published studies (Materials and Methods). When the input regulates a single downstream gene, both the maximum concentration of stressor that the population can survive and the population-level cost are similar for constant and pulsing inputs (Fig. 3 *A*). This result is expected, since the distribution of downstream proteins is equivalent for the two types of input (Fig. 2 *C*). However, when multiple genes are regulated together, populations with pulsing inputs are able to coordinate their response and survive higher concentrations of a toxic compound while maintaining equal costs (Fig. 3 *B*). Even modest benefits can provide a selective advantage, because they come with no added cost. Results for fast promoter binding dynamics (Fig. S4, *B* and *C*) and an alternative cost function (Fig. S2) are similar. Our results are consistent over a broad range of conditions, cost functions, and model parameters, indicating the generality of our findings. By coordinating downstream genes so that multiple stress-response mechanisms are engaged simultaneously, a pulsing input can achieve higher stress tolerance without added cost.

We note that the downstream genes modeled here all have high dissociation constants. This represents a conservative scenario; genes with lower K_D values or a mixture of downstream genes will exhibit greater benefits from coordination. We verified that downstream genes with higher affinity for the activator (lower K_D) achieve benefits from coordination (Fig. S6). In this case, the cost associated with input dynamics is lower due to the nonlinear nature of the activation curve. Therefore, input dynamics provide two benefits: frequently activated genes can enhance stress tolerance and also maintain a lower overall cost.

Nonperiodic pulsatile dynamics and extrinsic noise can coordinate downstream genes

Although we initially examined well-defined pulsatile signals to carefully control for pulse properties, we next asked whether our results could be generalized to other types of time-varying input. To test this, we used a model of the *E. coli* multiple antibiotic resistance activator (MarA) developed previously by our group (38). The multiple antibiotic resistance network is involved in protection against many stresses, including antibiotics, solvents, and other antimicrobial compounds (39,51). In this network, genes for the activator MarA and the repressor MarR are encoded in a single operon, which is regulated by both MarA and MarR, resulting in both positive and negative feedback controlling expression of the operon. Rapid increases in the level of MarA, followed by delayed inhibition by MarR may cause stochastic pulses in the expression of MarA (38). Once expressed, the regulator MarA activates over 40 genes with diverse K_D values, all of which exceed the mean concentration of the activator by at least an order of magnitude (39,52). We used this signal as an input to 40 representative downstream genes, selecting genes with a range of dissociation constants to match those measured in the literature (39) (Materials and Methods). We measured the maximum survivable concentration of an antibiotic stressor for a single gene and the suite of diverse downstream genes (Fig. 3, *C* and *D*). In each case, we compared the results to a model with a constant MarA input with a mean identical to that in the dynamic case. Consistent with our results using a well-defined pulse as an input, we found that stochastic pulses enable survival in higher concentrations of antibiotic stressors while maintaining similar or lower cost profiles.

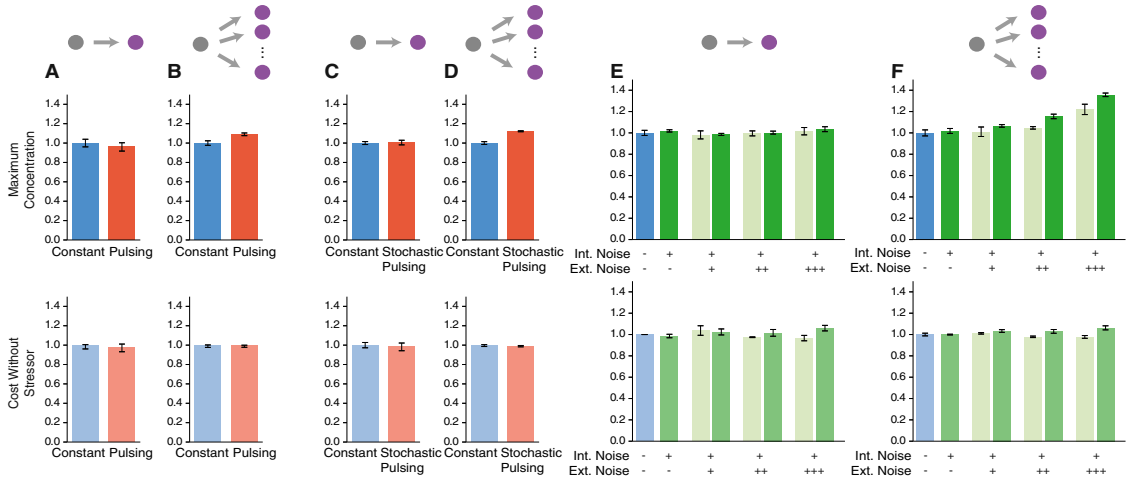

FIGURE 3 Coordination acts as a bet-hedging strategy with no added cost. (*A* and *B*) Maximum concentration of stressor that 0.1% of cells in a population can survive and the corresponding average cost of growing in the absence of stressor. Values were measured for constant and pulsing activator dynamics for one downstream gene (*A*) and 10 downstream genes (*B*), all with $K_D = 10{,}000$ molecules. (*C* and *D*) For the *mar* operon in *E. coli*, values were measured for constant and fluctuating MarA dynamics for one downstream gene with $K_D = 18{,}069$ molecules (*C*) and 40 downstream genes with experimentally derived dissociation constants (*D*) (see Materials and Methods). (*E* and *F*) Maximum survivable stressor and cost were measured for constant and fluctuating dynamics for different levels of noise in the activator and/or downstream genes for one downstream gene (*E*) and 10 downstream genes (*F*) with $K_D = 10{,}000$ molecules. Dark green bars show results with extrinsic and intrinsic noise in the activator and all downstream genes (cases with $\eta_{ext} = 0$, 0.11, 0.20, and 0.27 for the activator are shown). Light green bars show the contributions from extrinsic noise alone. For these simulations, there is no upstream activator, and downstream genes all have unique intrinsic noise and identical extrinsic noise signals. In all plots, values from the fluctuating dynamics are normalized to the constant input case. Error bars show standard deviations over three simulations. To see this figure in color, go online.

These results suggest that our findings on pulsatile inputs can be generalized to other dynamic regulators that control many downstream genes.

Noise in an upstream regulator has the potential to play a coordinating role if it is propagated to or affects all downstream genes in the same way (26,27). We considered both intrinsic and extrinsic noise sources in the input, where all genes are affected by unique intrinsic noise and identical extrinsic noise signals (12,26). We modeled extrinsic noise using an Ornstein-Uhlenbeck process and introduced fluctuations in the transcription-factor binding rate for all genes simultaneously, as in Shahrezaei et al. (40) (Materials and Methods). We calculated the maximum survivable stressor and the associated cost under increasing extrinsic noise. For regulation of a single downstream gene, adding extrinsic noise does not increase the maximum survivable stressor concentration (Fig. 3 *E*). However, when extrinsic noise affects multiple downstream genes, the coordination effect is visible (Fig. 3 *F*). In all cases, the cost is not highly impacted, so these gains are effectively free. Since extrinsic noise affects all genes simultaneously, it serves as a coordinating factor, which is combined with the noise dynamics introduced by the common upstream regulator; both contribute to the coordination of downstream genes (Fig. 3 *F*). This finding is consistent with experimental data on coordination in the yeast stress-responsive transcription factors Msn2/4 (11). Fluctuations in an upstream regulator provide a tunable mechanism to control coordinated stress response, and noise sources extrinsic to the stress-response pathway can add to this effect.

The timescale over which downstream genes remain coordinated is also important, as it determines whether beneficial effects will be passed on to daughter cells (53). To test this, we calculated the cross correlation between expression of downstream genes and found positive correlations that persisted well beyond the length of the cell cycle (Fig. S7). This timescale is sufficient for the activation of other resistance mechanisms that rely on sensing of the environment. Thus, input fluctuations can produce correlated expression of downstream genes over a timescale sufficient to produce resistant populations.

Dynamic inputs always outperform constant inputs in achieving coordination

We next asked what impact the number of stress response genes has on survival in the context of bet hedging. In cases where stress-response mechanisms are composed of several genes that work together to protect the cell, if these mechanisms are initiated by random events, then as the number of resistance genes goes up, the chances that they are coordinated at any given time goes down. We measured the

fraction of cells in a fixed size population that exhibit coordinated expression of downstream genes given different types of input (Fig. 4). For a single downstream gene, constant, pulsing, and noisy inputs are equally good, because there is no coordinating effect, but as the number of downstream genes increases, the benefit of input dynamics becomes apparent. Dynamics in the input play a coordinating role when there are multiple downstream genes, leading to a larger fraction of the population that can survive the sudden appearance of a stressor. If the promoters for downstream genes have higher affinity for the activator (lower K_D), a pulse in the input will frequently activate expression, resulting in cells with many coordinated downstream genes (Fig. S6 *D*). Therefore, the results for the high-K_D case shown in Fig. 4 are a conservative example of the benefits of input dynamics. Our findings are further supported by a simple mathematical model of input dynamics (Supporting Material).

CONCLUSIONS

The analysis presented here reveals an important role for noise and dynamics in inputs that control several infrequently activated downstream targets. Initiating expression of suites of stress-response genes in response to environmental signals might be too slow to deal with sudden catastrophic events. Diversifying phenotypes within a population before the crisis strikes can help ensure survival of a subset of the population (54). Such an approach is advantageous when the appearance of a stressor is rare and expression of stress-response machinery is costly.

Here, we asked about the scenario where stress response requires the coordinated action of several genes expressed simultaneously in a small fraction of the population. Examples where multiple mechanisms work in concert are common. Using a stochastic computational model, we examined the single-input-module regulatory motif, where one transcription factor regulates several downstream targets. In all cases, intrinsic noise in expression of the downstream genes leads to diversity within the population. However, if the upstream regulator is dynamic, for example, due to pulsatile expression or noise, it can drive coordination of diverse downstream target genes. Importantly, we found that even minor fluctuations in a transcription factor that regulates several target genes are sufficient to orchestrate coordination within a small subset of the population. Even for K_D values two orders of magnitude above the mean of the input, there is a measurable correlation with the dynamic input. We found that the overall cost with dynamic inputs is the same as or lower than that with constant inputs, and the maximum survivable concentration of stressor is the same or higher. Therefore, the benefits of coordination are in effect free. Because our findings test for rare events, only a small number of cells need to achieve coordination.

In contrast to strategies where two subpopulations of cells exist, as with bacterial persistence, coordination can allow for a graded response within the population. Because the activation of downstream gene expression is stochastic, there will be a distribution of stress-response phenotypes within the population, as opposed to an all-or-none response. In the future, it will be interesting to contrast the conditions under which distinct subpopulations and distributions each perform well and to compare these effects to sensory responses without stochastic effects (55).

The coordination of multiple downstream genes represents an alternative view on bet hedging to counter future environmental uncertainty. When the mean of the input is well below the dissociation constant of downstream genes, these genes are activated rarely. Most changes in input are filtered, but dynamic inputs ensure that when a downstream gene does turn on, it does so at a time when other genes may also be on. Here, we considered rare events, but we note that when the mean of the input is close to the dissociation constant of a downstream gene, fluctuations in the input are likely to be transmitted, resulting in well-coordinated outputs. Therefore, our simulations represent a conservative scenario for coordination. Regulators that control diverse suites of downstream genes will see benefits from coordination of multiple types of downstream genes. Overall, we found that dynamic and noise-driven coordination can play a bet-hedging role when multiple genes or stress-response mechanisms need to be coordinated without adding to the overall cost.

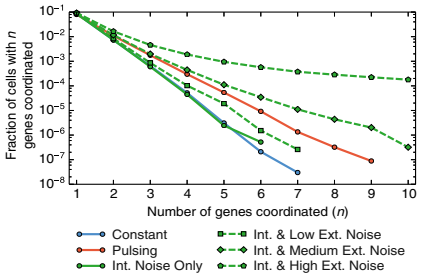

FIGURE 4 Fraction of cells with all downstream genes coordinated as a function of the number of downstream genes, *n*. The benefits of coordination from fluctuating input dynamics are more pronounced as the number of downstream genes increases. Note that in all cases, input dynamics provide higher levels of coordination than does a constant input. Increases in extrinsic noise increase coordination. Conditions show a different maximum number of coordinated genes because not all input cases are sufficient to ensure coordination within a set size of simulated population. To see this figure in color, go online.

SUPPORTING MATERIAL

Supporting Materials and Methods, Supporting Results, seven figures, and two tables are available at http://www.biophysj.org/biophysj/supplemental/S0006-3495(14)01233-8.

ACKNOWLEDGMENTS

We thank N. Rossi and T. Tomko for their critical reading of the manuscript. This research was supported by the National Institutes of Health (1R01AI102922) and by start-up funding from the University of Vermont.

REFERENCES

1. Fraser, D., and M. Kaern. 2009. A chance at survival: gene expression noise and phenotypic diversification strategies. *Mol. Microbiol.* 71: 1333–1340.
2. Balaban, N. Q., J. Merrin, …, S. Leibler. 2004. Bacterial persistence as a phenotypic switch. *Science.* 305:1622–1625.
3. Lewis, K. 2010. Persister cells. *Annu. Rev. Microbiol.* 64:357–372.
4. Süel, G. M., J. Garcia-Ojalvo, …, M. B. Elowitz. 2006. An excitable gene regulatory circuit induces transient cellular differentiation. *Nature.* 440:545–550.
5. Süel, G. M., R. P. Kulkarni, …, M. B. Elowitz. 2007. Tunability and noise dependence in differentiation dynamics. *Science.* 315:1716–1719.
6. Keren, I., N. Kaldalu, …, K. Lewis. 2004. Persister cells and tolerance to antimicrobials. *FEMS Microbiol. Lett.* 230:13–18.
7. Newman, J. R. S., S. Ghaemmaghami, …, J. S. Weissman. 2006. Single-cell proteomic analysis of *S. cerevisiae* reveals the architecture of biological noise. *Nature.* 441:840–846.
8. Blake, W. J., G. Balázsi, …, J. J. Collins. 2006. Phenotypic consequences of promoter-mediated transcriptional noise. *Mol. Cell.* 24: 853–865.
9. Arbel-Goren, R., A. Tal, …, J. Stavans. 2013. Effects of post-transcriptional regulation on phenotypic noise in *Escherichia coli*. *Nucleic Acids Res.* 41:4825–4834.
10. Neildez-Nguyen, T. M. A., A. Parisot, …, A. Paldi. 2008. Epigenetic gene expression noise and phenotypic diversification of clonal cell populations. *Differentiation.* 76:33–40.
11. Stewart-Ornstein, J., J. S. Weissman, and H. El-Samad. 2012. Cellular noise regulons underlie fluctuations in *Saccharomyces cerevisiae*. *Mol. Cell.* 45:483–493.
12. Elowitz, M. B., A. J. Levine, …, P. S. Swain. 2002. Stochastic gene expression in a single cell. *Science.* 297:1183–1186.
13. Levine, J. H., Y. Lin, and M. B. Elowitz. 2013. Functional roles of pulsing in genetic circuits. *Science.* 342:1193–1200.
14. Purvis, J. E., and G. Lahav. 2013. Encoding and decoding cellular information through signaling dynamics. *Cell.* 152:945–956.
15. Hao, N., and E. K. O'Shea. 2012. Signal-dependent dynamics of transcription factor translocation controls gene expression. *Nat. Struct. Mol. Biol.* 19:31–39.
16. Hansen, A. S., and E. K. O'Shea. 2013. Promoter decoding of transcription factor dynamics involves a trade-off between noise and control of gene expression. *Mol. Syst. Biol.* 9:704.
17. Cai, L., C. K. Dalal, and M. B. Elowitz. 2008. Frequency-modulated nuclear localization bursts coordinate gene regulation. *Nature.* 455: 485–490.
18. Wakamoto, Y., N. Dhar, …, J. D. McKinney. 2013. Dynamic persistence of antibiotic-stressed mycobacteria. *Science.* 339:91–95.
19. Charlebois, D. A., G. Balázsi, and M. Kærn. 2014. Coherent feedforward transcriptional regulatory motifs enhance drug resistance. *Phys. Rev. E Stat. Nonlin. Soft Matter Phys.* 89:052708.
20. Alon, U. 2007. Network motifs: theory and experimental approaches. *Nat. Rev. Genet.* 8:450–461.
21. Luscombe, N. M., M. M. Babu, …, M. Gerstein. 2004. Genomic analysis of regulatory network dynamics reveals large topological changes. *Nature.* 431:308–312.
22. Locke, J. C. W., J. W. Young, …, M. B. Elowitz. 2011. Stochastic pulse regulation in bacterial stress response. *Science.* 334:366–369.
23. Barbosa, T. M., and S. B. Levy. 2000. Differential expression of over 60 chromosomal genes in *Escherichia coli* by constitutive expression of MarA. *J. Bacteriol.* 182:3467–3474.
24. Martin, R. G., and J. L. Rosner. 2002. Genomics of the marA/soxS/rob regulon of *Escherichia coli*: identification of directly activated promoters by application of molecular genetics and informatics to microarray data. *Mol. Microbiol.* 44:1611–1624.
25. Dadiani, M., D. van Dijk, …, E. Segal. 2013. Two DNA-encoded strategies for increasing expression with opposing effects on promoter dynamics and transcriptional noise. *Genome Res.* 23:966–976.
26. Dunlop, M. J., R. S. Cox, 3rd, …, M. B. Elowitz. 2008. Regulatory activity revealed by dynamic correlations in gene expression noise. *Nat. Genet.* 40:1493–1498.
27. Munsky, B., G. Neuert, and A. van Oudenaarden. 2012. Using gene expression noise to understand gene regulation. *Science.* 336:183–187.
28. Boettiger, A. N. 2013. Analytic approaches to stochastic gene expression in multicellular systems. *Biophys. J.* 105:2629–2640.
29. Raj, A., and A. van Oudenaarden. 2008. Nature, nurture, or chance: stochastic gene expression and its consequences. *Cell.* 135:216–226.
30. Raj, A., C. S. Peskin, …, S. Tyagi. 2006. Stochastic mRNA synthesis in mammalian cells. *PLoS Biol.* 4:e309.
31. Megerle, J. A., G. Fritz, …, J. O. Rädler. 2008. Timing and dynamics of single cell gene expression in the arabinose utilization system. *Biophys. J.* 95:2103–2115.
32. Dekel, E., and U. Alon. 2005. Optimality and evolutionary tuning of the expression level of a protein. *Nature.* 436:588–592.
33. Wood, K. B., and P. Cluzel. 2012. Trade-offs between drug toxicity and benefit in the multi-antibiotic resistance system underlie optimal growth of *E. coli*. *BMC Syst. Biol.* 6:48.
34. Wood, K. B., K. C. Wood, …, P. Cluzel. 2014. Uncovering scaling laws to infer multidrug response of resistant microbes and cancer cells. *Cell Reports.* 6:1073–1084.
35. Gillespie, D. T. 1977. Exact stochastic simulation of coupled chemical-reactions. *J. Phys. Chem. A.* 81:2340–2361.
36. Bliss, C. I. 1939. The toxicity of poisons applied jointly. *Ann. Appl. Biol.* 26:585–615.
37. Greco, W. R., G. Bravo, and J. C. Parsons. 1995. The search for synergy: a critical review from a response surface perspective. *Pharmacol. Rev.* 47:331–385.
38. Garcia-Bernardo, J., and M. J. Dunlop. 2013. Tunable stochastic pulsing in the *Escherichia coli* multiple antibiotic resistance network from interlinked positive and negative feedback loops. *PLOS Comput. Biol.* 9:e1003229.
39. Martin, R. G., E. S. Bartlett, …, M. E. Wall. 2008. Activation of the *Escherichia coli* marA/soxS/rob regulon in response to transcriptional activator concentration. *J. Mol. Biol.* 380:278–284.
40. Shahrezaei, V., J. F. Ollivier, and P. S. Swain. 2008. Colored extrinsic fluctuations and stochastic gene expression. *Mol. Syst. Biol.* 4:196.
41. Gillespie, D. T. 1996. Exact numerical simulation of the Ornstein-Uhlenbeck process and its integral. *Phys. Rev. E Stat. Phys. Plasmas Fluids Relat. Interdiscip. Topics.* 54:2084–2091.
42. Rosenfeld, N., J. W. Young, …, M. B. Elowitz. 2005. Gene regulation at the single-cell level. *Science.* 307:1962–1965.
43. Fox, R. F., I. R. Gatland, …, G. Vemuri. 1988. Fast, accurate algorithm for numerical simulation of exponentially correlated colored noise. *Phys. Rev. A.* 38:5938–5940.
44. Peccoud, J., and B. Ycart. 1995. Markovian modeling of gene-product synthesis. *Theor. Popul. Biol.* 48:222–234.
45. Larson, D. R. 2011. What do expression dynamics tell us about the mechanism of transcription? *Curr. Opin. Genet. Dev.* 21:591–599.
46. Kaern, M., T. C. Elston, …, J. J. Collins. 2005. Stochasticity in gene expression: from theories to phenotypes. *Nat. Rev. Genet.* 6:451–464.
47. Lee, P., B.-R. Cho, …, J.-S. Hahn. 2008. Yeast Yak1 kinase, a bridge between PKA and stress-responsive transcription factors, Hsf1 and Msn2/Msn4. *Mol. Microbiol.* 70:882–895.

48. Sakurai, H., and Y. Enoki. 2010. Novel aspects of heat shock factors: DNA recognition, chromatin modulation and gene expression. *FEBS J.* 277:4140–4149.

49. Tay, S., J. J. Hughey, …, M. W. Covert. 2010. Single-cell NF-kappaB dynamics reveal digital activation and analogue information processing. *Nature.* 466:267–271.

50. Ashall, L., C. A. Horton, …, M. R. H. White. 2009. Pulsatile stimulation determines timing and specificity of NF-kB-dependent transcription. *Science.* 324:242–246.

51. Martin, R. G., and J. L. Rosner. 2004. Transcriptional and translational regulation of the marRAB multiple antibiotic resistance operon in *Escherichia coli*. *Mol. Microbiol.* 53:183–191.

52. Wall, M. E., D. A. Markowitz, …, R. G. Martin. 2009. Model of transcriptional activation by MarA in *Escherichia coli*. *PLOS Comput. Biol.* 5:e1000614.

53. Charlebois, D. A., N. Abdennur, and M. Kaern. 2011. Gene expression noise facilitates adaptation and drug resistance independently of mutation. *Phys. Rev. Lett.* 107:218101.

54. Davidson, C. J., and M. G. Surette. 2008. Individuality in bacteria. *Annu. Rev. Genet.* 42:253–268.

55. Kussell, E., R. Kishony, …, S. Leibler. 2005. Bacterial persistence: a model of survival in changing environments. *Genetics.* 169:1807–1814.

2.2 Phenotypic diversity using bimodal and unimodal expression of stress response proteins in fluctuating environments

Javier Garcia-Bernardo[1],Mary J. Dunlop[2,*]

[1] Department of Computer Science, [2] School of Engineering, University of Vermont, USA. * corresponding author: mjdunlop@uvm.edu

Abstract

Populations of cells need to express proteins to survive the sudden appearance of stressors. However, these mechanisms may be taxing, restricting how frequently they can be used. To survive in changing environments, organisms can devote part of the population towards expressing these proteins, allowing individual cells to stochastically switch between fast-growing and stress-tolerant states. One way to diversify the population is to use genetic networks coupled with noise to generate bimodal distributions with two distinct subpopulations, each adapted to a stress condition. Another survival strategy is to rely on random fluctuation in gene expression to produce continuous, unimodal distributions of the stress response protein. In both cases, some fraction of the population must always express high enough levels of protein to hedge against the sudden appearance of a stressor. To quantify the environmental conditions where bimodal versus unimodal expression is beneficial, we used an evolutionary algorithm to evolve optimal or near-optimal distributions of stress response proteins given environments with sudden fluctuations

between low and high stress. We found that bimodality is evolved for a large range of environmental conditions. When cells can sense and adapt to the environment, the parameter region where bimodal expression is favored increases further. However, we asked whether these findings were an artifact of considering stress environments with two well-defined conditions (low and high stress). We found that as noise in the environment increases, or when the cells must cope with an intermediate environment (medium stress), the benefits of bimodality decrease. Overall, our results indicate that although bimodal distributions of proteins can be beneficial when there are two clearly defined stress states, under realistic conditions with noise in the environment or multiple stress levels, a continuum of resistance phenotypes generated through a unimodal distribution is sufficient to ensure survival without a high cost to the population.

Introduction

Populations of cells that live in fluctuating environments must cope with a wide range of conditions and sudden changes in their surroundings. Cells can sense their environment and respond to changes. However, if the time required to initiate a response is longer than the time the stressor takes to act, cells need alternative strategies to ensure that the entire population is not killed off due to the sudden appearance of a stressor. Furthermore, initiating stress response mechanisms in all cells within a population may be costly. When sensing the environment is too slow or too costly, populations can rely on genetic and phenotypic variation to balance survival and growth. For example, they may sacrifice growth in low stress conditions to increase fitness in other environments (1–3). In the past decade bet hedging, a type of non-genetic variation between individuals, has gained

attention for its role in multiple biological processes (1, 3). For instance, the presence of subpopulations of non-growing persister cells allows bacterial populations to survive high concentration of antibiotics that target cell growth (4). This persistent population has been found in numerous pathogenic microbes, and has been shown to be an important contributor to antibiotic resistance (5). Similarly, under nutrient limitation, *Bacillus subtilis* generates phenotypic diversity resulting in normally growing cells, cells that sporulate, and those that become competent (6, 7). Maintaining different phenotypes within the same genotype allows populations of cells to ensure variability at every generation, reducing differences in the population growth rate across environments and ensuring survival under a variety of conditions (8).

In this paper, we focus on how a population of cells grows in the presence of a time-varying stressor. Cells can express genes to tolerate high concentrations of a stressor, such as genes encoding efflux pumps, reductases, and DNA repair systems (9). However, these stress response mechanisms can have a high metabolic cost (10). Thus, populations may use phenotypic diversity so that not all cells have the burden of expressing them. Two approaches include: (i) The generation of two distinct phenotypic states optimized for each environment, which we refer to as a bimodal distribution. Establishing two well-defined phenotypes and stochastically switching between them can be advantageous in some conditions. For instance, in bacterial persistence populations are bimodal, maintaining a small subpopulation of dormant cells in addition to normally growing cells (11). This type of bet-hedging has been evolved in *Pseudomonas fluorescens* in the presence of alternating stresses (12, 13). (ii) An alternative approach is to generate a continuum of stress resistance levels within a population, which we refer to as a unimodal distribution. In this case, cells have a similar phenotype with variations about the mean levels. In contrast to the bimodal

case, there are not distinct phenotypic states. An example of unimodal distributions comes from TATA box-containing genes associated with stress response in *Saccharomyces cerevisiae*, which exhibit large levels of variability that protect against future environmental changes (14). Similarly, increased population heterogeneity has been shown to enhance survival of stress in *S. cerevisiae* (15). A broad, continuous distribution of phenotypes has also been evolved in *Escherichia coli* in a periodic selection and mutation experiment (16). Phenotypic diversity, in the form of bimodal or unimodal distributions of phenotypes, plays an important role in increasing fitness in uncertain environments.

The mathematical analysis of fluctuating environments dates back to work by Levins, who showed that environmental fluctuations hinder adaptation to a single phenotype (17). Since then, many studies have examined the relationship between time-varying environments and cellular phenotypes. Generally, cells are modeled as growing exponentially, with each phenotype having a distinct growth rate for each environment and a rate of switching to other phenotypes (18–23). Given the large number of parameters present, numerical and analytical studies have primarily focused on the case with two environments and two phenotypes, with the following general conclusions: Two different optimal strategies can be found, where the optimum depends on the frequency at which the environment changes. A unimodal population is best for very rapid or very slow environmental changes, and a bimodal population where cells stochastically switch between two phenotypes is best for intermediate ranges of environmental switching (24). Furthermore, the unimodal population can be either adapted to the current environment if the changes are slow, i.e. cells can sense and adapt to the extracellular conditions; or adapted to the mean environment if the changes are rapid (24). When cells do not explicitly sense their environment, bimodal strategies with stochastic switching between the two states are

favored (20). Even in conditions where cells do sense their environment, bimodality can still be used to prevent complete extinction of the population if sensing is too slow (25, 26) In general, in a periodic environment, the optimal switching rate between phenotypes in a bimodal population is proportional to the asymmetry of the stress environment (25) and the transition rate between environmental states (18, 27). These results have provided insight into the cases where bimodal populations are favored, showing that bimodality coupled with stochastic switching between states is advantageous for a large range of conditions.

Although these studies have demonstrated the theoretical benefit of bimodality, more than 99% of *E. coli* genes show unimodal distributions in their protein levels (28). There are select examples of bimodal gene expression in *E. coli*, but relatively few cases exist; other bacterial species appear to be similar (29). Thus, we were motivated to understand the conditions where bimodal distributions of proteins increase the growth rate of a population with respect to a unimodal distribution. To achieve this, we developed a computational model and used a differential evolution algorithm (30) to evolve optimal or near-optimal distributions of phenotypes for a population growing in the presence of a time-varying stressor. When we restricted the concentration of the stressor to two levels (low and high), we were able to reproduce the benefits of bimodality previously reported. However, this benefit disappeared when variability in the concentration of the stressor was increased. This was the case when there was noise in the environment, or when there were more than two distinct environmental conditions. Given realistic conditions, unimodal distribution of proteins may be a straightforward bet hedging approach for surviving in fluctuating environments.

Results

Protein expression model and environmental variables To study how populations of cells optimize growth in the presence of fluctuations in the concentration of a stressor in the environment, we developed a model where a protein controls the level of resistance to the stressor. For example, this could be a regulatory protein that controls expression of a suite of downstream genes involved in stress response, or it could provide stress resistance directly; examples include efflux pumps or proteins that induce growth arrest to evade antibiotics. In the model, increased protein expression allows for survival in high stress environments, but impacts growth in low stress environments since expression places a burden on the cell. We used an evolutionary algorithm to find optimal or near-optimal distributions of protein levels in the population given a fluctuating environment as an input. Because we evolve the distributions directly, we do not explicitly model switching or specify the method by which the distributions are generated. Initially, we restricted the distribution of proteins to be the weighted sum of two gamma distributions, which can represent either unimodal or bimodal expression of proteins, depending on weighting values (Fig. 2.5A). We later relaxed this restriction and obtained similar results, as discussed below. A gamma distribution arises from a two-state model of gene expression, where the promoter can be ON or OFF and the protein is expressed in bursts (31). We used the evolutionary algorithm to select the shape and rate parameters of the distributions (Methods). It is possible for the evolutionary algorithm to evolve tight distributions, where there is very little variation in protein levels or broad distributions, where there is wide variation. We chose the upper and lower limits of the gamma distribution parameters to match *in vivo* values measured in bacteria (28). Importantly, we note that it is

possible to evolve parameters such that the two gamma distributions collapse to a unimodal distribution. For example, if the weight of the second gamma distribution is zero, there will be only a single, unimodal population. Thus, the weighted sum of two gamma distributions allows a flexible representation where both unimodal and bimodal protein distributions with broad or narrow distributions can be evolved.

We also compared the ability of cells to sense environmental changes. In the case where cells cannot sense stress levels (Fig. 2.5B), a bimodal population of cells grows well in the low stress environment, with cells in the low protein expression state growing faster than those in the high protein expression state. Individual cells within the population stochastically switch between the two states. When the environment changes and cells enter the high stress conditions, all the cells in the low expression state die off, but those with high expression survive. Because the cells do not sense their environment they continue to stochastically switch between phenotypic states. When this happens in the high stress environment, the cells that enter the low protein phenotype die. When conditions switch back to the low stress environment, the population can regrow, again with stochastic switching between the two phenotypic states. The sensing case is similar (Fig. 2.5C), but once cells are in the high stress environment they sense their conditions and do not switch to the low protein phenotype. The underlying protein distributions are shown in Figs. 2.5B–C. In low stress conditions, the population exhibits a bimodal distribution with stochastic switching regardless of whether there is sensing or not. This is required, even with sensing, because we assume that the time required to sense and respond to a stress is long enough that any cells in the low protein phenotype will be killed by the stressor. The difference between the no sensing and sensing cases appears in the high stress conditions, where cells that can sense have no reason to switch to the low protein phenotype.

We also tested a broad range of environmental transition properties. We modified the ratio between the time spent in high and low stress (Fig. 2.5D) and the environmental transition rate (Fig. 2.5E). See Methods for a full description of the model and parameters.

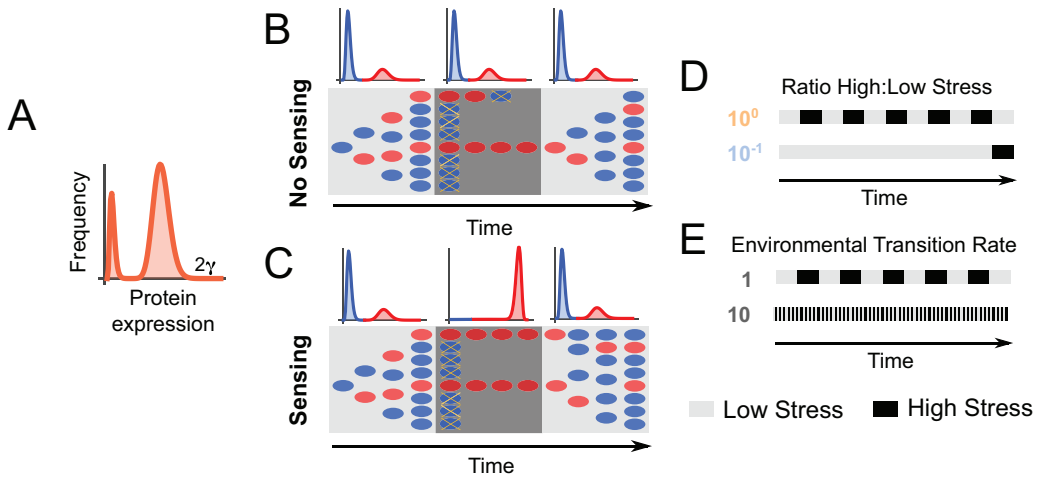

Figure 2.5: **P2. Population and environmental variables tested.** (A) The distribution of protein levels in the population was initially restricted to be a weighted sum of two gamma distributions. (B) Environments vary between low and high stress. Without sensing, the population always maintains cells with low and high levels of protein expression (histograms), where cells switch stochastically between these two phenotypic states. Under low stress, cells with low protein expression (blue) grow well, while cells with high protein expression (red) grow slowly due to the burden of expressing the stress response protein. Under high stress, cells with low protein expression are killed (yellow x's), while cells with high protein expression survive. Note that the histograms are colored as blue and red to distinguish cells with low and high expression, however all cells are part of the same bimodal distribution. (C) With sensing, populations maintain diversity as a bet hedging strategy when stress levels are low. When stress levels are high, all surviving cells remain in the high protein state. (D) Cartoon showing ratio between the time spent in high and low stress. (E) Cartoon showing the environmental transition rate. Note that the ratio of high to low stress is identical for both transition rates shown.

Bimodality is evolved for a wide range of environmental conditions Initially, we tested different environmental conditions, varying both the ratio of high to low stress and the

rate of transition between environmental states. For each pair of values, we used the evolutionary algorithm to optimize the distribution of protein levels. We then recorded the relative sizes of the two evolved gamma distributions, comparing the ratio of cells exhibiting the high protein expression phenotype to the low protein phenotype. We found that two strategies were evolved: either the entire population was adapted to the high stress condition (darkest purple in Figs. 2.6A–B) or a bimodal population with a resistant subpopulation appeared (light purple). A unimodal population with low protein expression (white) was never evolved, since resistant cells are required to survive the transition from low to high stress. With no sensing, bimodal distributions are evolved in the cases where the ratio of high to low stress is small because most of the time cells are in low stress conditions with rare excursions to the high stress environment (Fig. 2.6A). The fraction of resistant cells depends only on the ratio of the stresses, and not on the environmental transition rate. This is because the growth rate of a population without sensing is constant for each stress condition, in contrast with the sensing case, where the growth rate changes during the time in high stress conditions as the cells adapt (Fig. 2.6B). With sensing, the population can afford to lose a higher fraction of cells due to the sudden appearance of the stressor, since the remaining cells will adapt to the stress. Thus, with sensing a higher fraction of the population can be devoted towards growing well in low stress, and bimodality is evolved under most environmental conditions.

To quantify the benefit of sensing, we measured the growth rate for populations of cells that were allowed to sense the environment, and for populations where sensing was prohibited. In all cases, sensing outperformed no sensing. However, the degree to which there was a benefit to sensing depended upon the ratio of high to low stress in

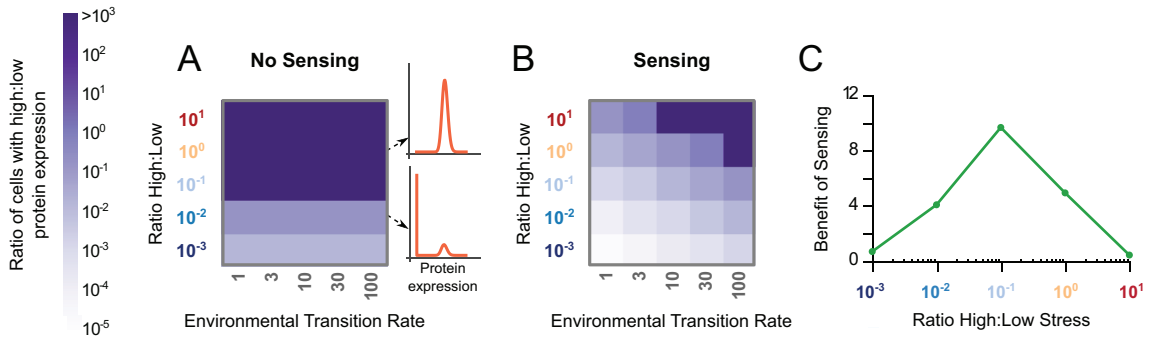

Figure 2.6: **P2. Bimodality is evolved in many environmental conditions**. (A, B) The ratio of cells with high to low protein expression is plotted as a function the ratio of high to low stress and the environmental transition rate. Representative protein histograms show unimodal (dark purple) and bimodal (light purple) distributions. (A) For populations with no sensing, bimodality is evolved when the ratio of high to low stress is small. (B) For populations with sensing, bimodality is evolved for a large region of environmental parameters and depends on both the ratio of stress conditions and the environmental transition rate. (C) The benefit of sensing is plotted as a function of the ratio of high to low stress, reaching its maximum for moderately asymmetric environments. The benefit is measured as the difference in growth rate between the sensing and no sensing populations (Supporting Text and Fig. B.1). These simulations use an environmental transition rate of 10.

the environment (Fig. 2.6C). In the extreme cases where cells are mostly in stressed or unstressed environments, there is little advantage to sensing since conditions are well known. In contrast, when the time spent in each environment is symmetric, sensing has a distinct advantage. The highest benefit to sensing is achieved for moderately asymmetric environments, where the optimal strategy for the no sensing population is a unimodal distribution with high protein levels, while the sensing population can rely on a bimodal distribution of phenotypes. The metric we use here to measure the benefit of sensing can be translated into the amount of time it would take a population with sensing to overtake a population without sensing in a competitive growth experiment (Supporting Text and Fig. B.1).

We next relaxed our requirement that the protein distribution be the weighted sum of two gamma distributions. We allowed the evolution of any type of distribution with no restrictions, finding equivalent results to the two gamma distribution case (Fig. B.2). For the case of two well-defined environments, we found that bimodality is evolved for a large range of fluctuating environments.

In our initial tests, we assumed that the stressor was strong enough that it killed off all cells with low protein expression. We next asked whether our results were dependent on whether the stressor was weak or strong. We define a weak stressor as a toxin that inhibits cell growth for cells that do not have high levels of protein expression, in contrast to a strong stressor that kills these cells (Supporting Text). When they target bacteria, weak stressors are known as bacteriostatic and strong stressors are bacteriocidal. Our results with weak stressors show that with no sensing, the evolved strategy is unimodal for nearly all environmental conditions (Fig. B.1). Populations have low protein expression for all but the largest ratio of high to low stress. This corresponds to the case where the cells stay latent until the stressor has passed. A unimodal distribution with high protein expression is evolved only when the time spent in high stress conditions is large. Between these two survival strategies, i.e. unimodal adapted to low stress and unimodal adapted to high stress, bimodality is evolved for a very small region of the environmental parameter space. For the case with sensing, the optimal strategy is always to stay latent until the stressor is sensed. This is expected since the stressor only inhibits growth, and thus it is possible to adapt to it even if the toxin appears abruptly. Because the growth rate in high stress conditions is very small even when the population is perfectly adapted, staying latent is almost as good as adapting to the stress. Therefore the benefit of sensing is lower than in the case with a strong stressor, where cells die off if they do not adapt to the stress conditions. The

evolved distributions with no restriction have equivalent results. Consistent with previous findings (32), our results show that bimodality is primarily beneficial when the strength of the stressor is strong.

Bimodality is beneficial for populations of cells growing in two well-defined stress conditions We next asked under what environmental conditions bimodal populations outperform unimodal populations. To do this, we evolved distributions by restricting protein levels to follow either two weighted gamma distributions as before (we refer to this as 2γ), or one gamma distribution (1γ), as shown in Fig. 2.7A. We evolved the optimal distributions for 1γ and 2γ given identical stress environments. Since it is possible for the 2γ distribution to recover a single gamma distribution, the 2γ case is always better than or equal to the 1γ case. We calculated the growth rate for the evolved strategies with the 1γ and 2γ restrictions as a function of the ratio of high to low stress and the environmental transition rate. For the no sensing case, the optimal strategy depends only on the ratio of the stresses. When the ratio of high to low stress is large, the optimal strategy for both the 1γ and 2γ cases is a unimodal distribution adapted to high stress, so there is no benefit to bimodality. As the stress ratio decreases, there is a sudden transition where the 2γ distribution switches from a unimodal population to a bimodal population containing a subpopulation of cells with high protein expression while most cells have low expression. In order for the 1γ case to maintain a sufficient number of cells in the high protein phenotype under the same environmental conditions, many cells must express intermediate protein levels. Cells with intermediate protein expression provide no benefit to the population because they are not capable of surviving sudden stress, but also impose a modest burden on the growth of the population. As the stress ratio is further reduced,

the difference between the two distributions diminishes as fewer cells need to maintain a high protein phenotype. This phenomenon is visible in the examples of evolved histograms (Fig. 2.7B).

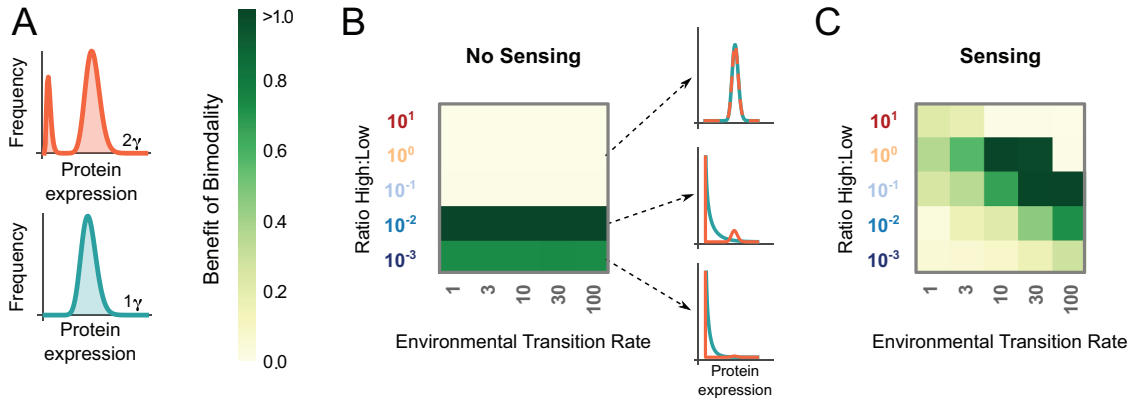

Figure 2.7: **P2. Bimodality provides higher fitness than unimodality when the environment has two alternating states.** (A) We compared conditions where we restricted protein levels to be either the weighted sum of two gamma distributions (2γ) or a single gamma distribution (1γ). (B, C) The benefit of bimodality is plotted as a function of the ratio of high to low stress and the environmental transition rate. (B) For populations with no sensing, there is a benefit to bimodality when the ratio of high to low stress is small, which is reflected in differences in the evolved distributions. (C) For populations with sensing, the benefit of bimodality depends on both the ratio of high to low stress and the environmental transition rate. The benefit is measured as the difference in growth rate between the strategies evolved with 2γ and 1γ restrictions (Supporting Text and Fig. B.1).

For the sensing case, bimodality is beneficial in environments with relatively symmetric levels of high and low stress (Fig. 2.7C). Since the population is able to adapt to high stress conditions, the evolved distribution depends now on the time spent in low stress conditions and the number of transition events. Therefore, the benefit depends on both the ratio of stresses and the environmental transition rate. In Fig. 2.6, we show that sensing increases the parameter region where bimodality is evolved. However, when the population is able to sense the environment, the growth in high stress conditions is equal for both the unimodal

and bimodal cases, since they adapt to the stress in an identical way. Therefore, the benefit of bimodality is generally lower, though still positive, for sensing populations than for populations without sensing.

Increased variability in the environment decreases the benefit of bimodality Although we found that bimodal distributions outperform unimodal distributions for a wide range of environmental conditions, we wondered whether this effect was due to the binary nature of the stresses (either low or high). We hypothesized that variability in the environment would decrease the benefit of bimodality. To test this, we introduced noise in the two stress levels (Methods, Fig. 2.8A) and recalculated the benefit of bimodality, quantifying the difference in growth rates between the evolved distributions with the 2γ and 1γ restrictions. As noise increases, strategies with more cells in the elevated protein expression state are favored because less time is spent in the complete absence of a stressor. For the highest levels of noise, both 1γ and 2γ cases evolve unimodal distributions (Fig. B.4). Consequently, we found that for both no sensing and sensing populations (Figs. 2.8B–C), the benefit of bimodality decreased as noise in the environment increased.

We also asked whether considering only two stress environments was leading to the observed benefits in bimodality. To test this, we increased the number of environmental states by adding an environment with medium stress and measured the benefit of bimodality as a function of the time spent in this intermediate environment (Fig. 2.8D). Similar to simulations with increasing levels of noise, we found that for both no sensing and sensing populations (Figs. 2.8E–F), the benefit of bimodality decreased as the time in the intermediate environment increased. Two factors contribute to this decrease: First, if the cells are not able to sense their surroundings, both 1γ and 2γ cases evolve identical

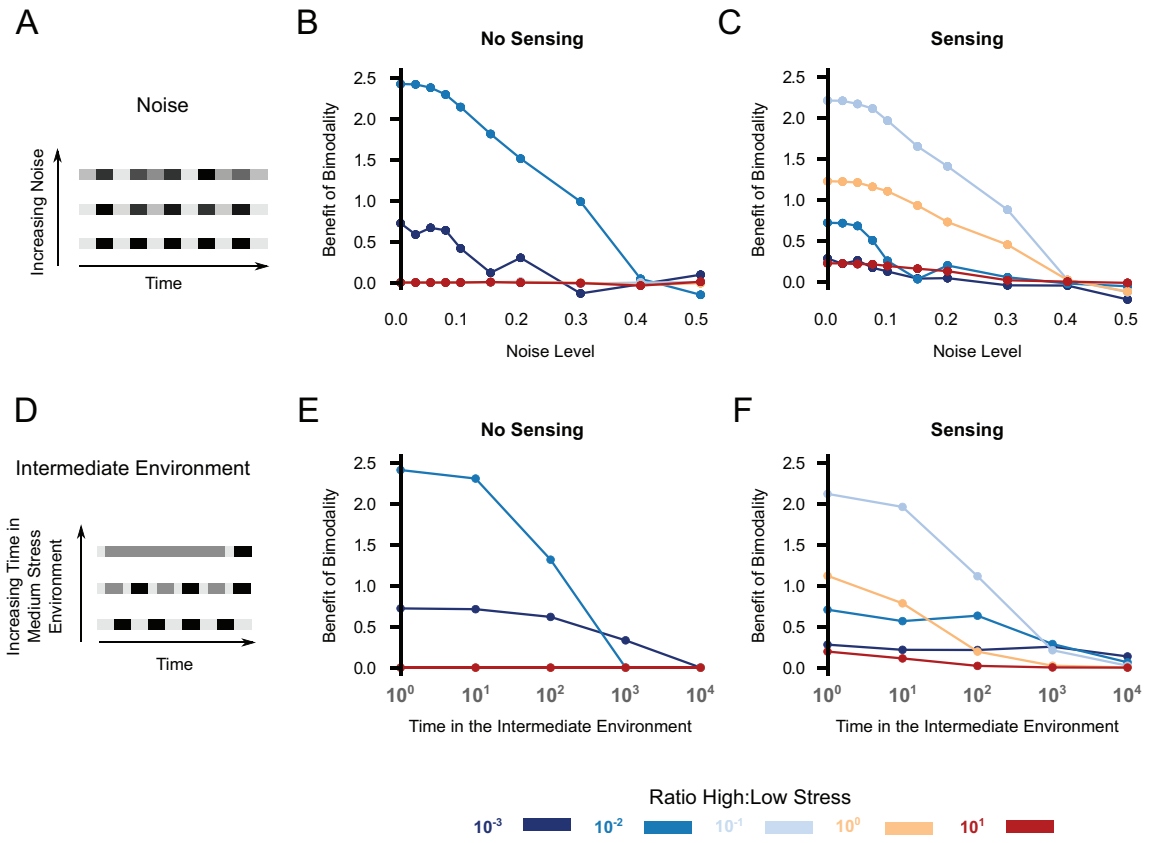

Figure 2.8: **P2. The benefit of bimodality is reduced when environmental variation increases.** (A) Cartoon showing increasing noise in the stress levels. (B, C) The benefit of bimodality is reduced for both (B) no sensing and (C) sensing populations as noise increases. Dots correspond to the replicate with highest evolved growth rate out of three independent simulations (Methods). (D) Cartoon showing the presence of an intermediate, medium stress environment. (E, F) The benefit of bimodality is reduced for both (E) no sensing and (F) sensing populations as the time in the intermediate environment increases. In (B) and (E), the benefit results for stress ratios 10^{-1} to 10^{1} are all zero, and thus are hidden behind the 10^{1} line.

unimodal distributions when the time in the medium stress environment is large (Fig. B.4). Second, if the cells are able to sense and adapt to the environment, the growth rate in medium stress conditions is identical for both the 1γ and 2γ cases since cells adapt perfectly to the medium stress condition, therefore the evolved distribution does not

depend on the time spent in the medium stress environment. Thus, we find that under realistic scenarios, such as environments with noise or more than two discrete stress levels, unimodal distributions perform just as well as bimodal distributions.

We finally asked whether using the 2γ distribution was limiting how well the evolved strategies could perform in the intermediate environment. In principle, a trimodal distribution could provide the optimal conditions for three environments. To test this, we removed the 2γ restriction and allowed the distribution to evolve freely without any requirements on its shape. Even under these non-restrictive conditions, the populations evolved only unimodal or bimodal distributions (Fig. B.5). This is because the intermediate environment acts as a weak stressor, where bimodality is only evolved for a small range of parameters (Fig. B.1). In fluctuating environments the advantage of bimodality comes from the ability to survive the sudden transition from low to high stress, which is not necessary for an intermediate stress state. Therefore, even with more than two distinct stress levels, it is only necessary to evolve two levels of protein expression: one that ensures survival in the highest level of stress and a second that optimizes growth in low stress.

Conclusions

Populations of cells live in the presence of intermittent, time-varying stressors. Cells have mechanisms to survive the appearance of a stressor, however the cost associated with stress resistance can be high. Thus, cells need to balance high growth rates in the absence of the stressor with high survival rates when a stressor appears abruptly in the environment. A possible strategy is to diversify the population, allowing some cells to grow well when no stress is present, while some have high enough protein expression that they can survive

stress, hedging against the sudden appearance of a stressor. Phenotypic diversity within the population can be achieved through multimodal distributions of protein levels, or through a broad, continuous distribution of proteins.

Here, we compared bimodal and unimodal distributions that can result from diversity in gene expression, asking under what conditions bimodality is beneficial. We used an evolutionary algorithm to evolve optimal or near-optimal distributions of proteins for different environmental conditions. We varied the time spent in high and low stress, the environmental transition rate, the sensing capabilities of the cells, noise in the concentration of the stressor, and the number of stress levels. Since protein expression typically follows a gamma distribution *in vivo*, we initially restricted the evolved distributions to be either a single gamma distribution or the weighted sum of two gamma distributions. We used the difference in growth rate between the two alternatives to assess the benefit of bimodality, finding that while bimodality is evolved for a wide range of conditions if the environment has only two well-defined states, this benefit disappeared in the presence of noise or when the time spent in an intermediate environmental state increased.

Our results raise the question of what benefits are provided by bimodality, given realistic environmental conditions. One benefit may be longer autocorrelation times in the protein levels that bimodality can provide. Unimodal distributions in stress resistance levels can be the result of random fluctuations in gene expression (31). The half-life of these fluctuations is typically one to three generations (33, 34). On the contrary, the time spent in each phenotypic state with a bimodal system can be large, extending for many generations (35). An example of bimodal protein expression in *E. coli* is persistence, where fewer than 1% of cells in the population are in a resistant, non-growing state that is tolerant to antibiotics (4). The switch between the growing and latent states is stochastic, and cells can stay in each

state for many generations (36, 37). The advantage of bimodality in this case may come from the extended time the cells spend in the resistant state. One alternative to bimodality that could achieve longer stress resistance times would be to couple a unimodal distribution with sensing. In this case, cells could use noisy gene expression to survive a sudden stress shock, and then adapt to it. However, maintaing the sensing machinery may be costly if the stressor is only rarely encountered.

In this study, we evolved distributions of protein levels, however our results do not specify how these distributions are achieved. Bimodality can be generated by genetic networks, such as through the use of positive feedback networks (35). The presence of these additional genetic control elements can add evolutionary and maintenance costs, which we have not included in our model. Unimodal distributions are more straightforward to generate, as noise in gene expression is sufficient to produce a continuum of resistance levels (35). In general, if the cost of maintaining the architecture required to generate bimodal distributions is higher than the benefit acquired, bimodality will not be evolved. In the future it will be interesting to link the regulatory architecture required to generate protein distributions to the results presented here.

We conclude that bimodal protein expression patterns can be beneficial under certain conditions, such as when environmental states are well-defined and the number of states is small. However, under realistic environmental conditions with noise and uncertainty in stress levels, unimodal protein distributions are often sufficient to provide diversity within the population that can ensure survival.

Methods

Distribution of protein levels In the context of general stress response, some proteins confer resistance to a broad range of chemicals, either by regulating expression of suites of genes or by directly providing stress resistance. Therefore, we represented the phenotype of a cell, P, as the concentration of a hypothetical protein involved in response to stress. To study populations of cells growing in fluctuating environments, we developed a model that assigns fitness values (growth rates) to a distribution of protein levels in a series of environments. We evolved the probability distribution of the protein under the basal conditions, where no stressor was present. This distribution is encoded by a n-dimensional vector, where the dimension corresponds to different protein levels in the population, and the n values correspond to the probability of expressing the phenotypes, $p(P)$. The values of P were set to n bins: $\{0-100, 100-200, ..., 9900-10000\}$ molecules, to represent a typical range of protein numbers that can be found in both bacteria and yeast (38).

Gamma distributions The n values in vector $p(P)$, were extracted from a gamma distribution in the 1γ case, the weighted sum of two gamma distributions in the 2γ case, or evolved directly in the case with no restrictions.

For the 1γ case

$$p(P) = \frac{b^a}{\Gamma(a)} P^{a-1} e^{-bP}, \tag{2.1}$$

where the values a (shape parameter) and b (rate parameter) define the distribution. The 1γ case has two parameters that are evolved in the differential evolution algorithm: a and b.

For the 2γ case

$$p(P) = w_1 \frac{b_1^{a_1}}{\Gamma(a_1)} P^{a_1-1} e^{-b_1 P} + w_2 \frac{b_2^{a_2}}{\Gamma(a_2)} P^{a_2-1} e^{-b_2 P}, \tag{2.2}$$

where w_1 and w_2 set the relative weights of the two gamma distributions. The 2γ case has six parameters that are evolved: a_1, b_1, w_1, a_2, b_2, and w_2.

For the free case $p(P)$ is evolved directly, so there are n parameters evolved.

For each of the three cases, the distributions are normalized such that $\sum_P p(P) = 1$, where P corresponds to the protein levels $\{0-100, 100-200, ..., 9900-10000\}$ molecules.

Environmental parameters The concentration of the stressor, S, and the time spent in the different stress levels characterize the environment. For the case with two environmental states, the concentrations of the stressor were set to 0mM (low stress) and 10mM (high stress). The time spent in the two environments, measured in generations, is shown in Table 2.1.

	Environmental Transition Rate				
Ratio High:Low	1	3	10	30	100
10^1	1,000:100	333:33	100:10	33:3	10:1
10^0	1,000:1,000	333:333	100:100	33:33	10:10
10^{-1}	1,000:10,000	333:3,333	100:1,000	33:333	10:100
10^{-2}	1,000:100,000	333:33,333	100:10,000	33:3333	10:1,000
10^{-3}	1,000:1,000,000	333:333,333	100:100,000	33:33,333	10:10,000

Table 2.1: **Time spent in low and high stress conditions**. For each ratio of high to low stress and environmental transition rate, the number of generations spent in each state is shown. The format of the table entries is time in high:low stress.

Cost and benefit We used the cost-benefit function described in (39), which is based on (10, 40). Briefly, the growth rate of a cell, $\lambda_{P,S}$, is defined in terms of $c(P, S)$, where

$$c(P, S) = c_1(P) + c_2(P, S) - c_1(P)c_2(P, S). \tag{2.3}$$

$c(P, S)$ is the cost of growing when the concentration of stressor in the environment is S and the intracellular number of proteins is P. $c_1(P)$ corresponds to the cost of expressing the stress resistance machinery at a level P, while $c_2(P, S)$ is the cost of growing in the presence of a concentration of stressor S given a stress resistance level P.

$$\begin{aligned} c_1(P) &= \frac{n_0 P}{1 - P/M} && (2.4)\\ c_2(P, S) &= \frac{S_{eff}^n}{k^n + S_{eff}^n} && (2.5)\\ S_{eff} &= \frac{S}{1 + B} && (2.6)\\ B &= \frac{b_{max} P}{k_b + P}, && (2.7) \end{aligned}$$

where $M = 15,000$ molecules, $n_0 = 10^{-5}$, $k = 1$mM, $n = 2$, $b_{max} = 10$, and $k_b = 15,000$ molecules. See (39) for a complete description of the equations and parameters.

Using the cost, we defined the growth rate as

$$\lambda_{P,S} = \begin{cases} \frac{c_{th} - c(P,S)}{c_{th}} & \text{if } c(P, S) < c_{th} \\ -1 & \text{if } c(P, S) \geq c_{th}. \end{cases} \tag{2.8}$$

Note that $\lambda_{P,S}$ is normalized to maintain growth rates between 0 and 1 when the cost is under the threshold c_{th}. $\lambda_{P,S} = 1$ is the maximal growth rate; positive values less than this

indicate slow growth. $\lambda_{P,S} = -1$ corresponds to the cell dying in one generation. We set $c_{th} = 0.9$, however the results are not specific to the exact value used.

Fitness function The fitness of a population with a distribution of protein levels is measured by the overall growth rate. We assumed that in a given environmental condition, the distribution of protein levels is at equilibrium (20) (Supporting Text). At equilibrium, the growth of a population depends on the fraction of cells at each protein level. The ratio of final to initial number of cells in one generation is

$$N_1/N_0 = \sum_P x_P 2^{\lambda_{P,S}}, \tag{2.9}$$

where N_0 and N_1 are the initial number of cells and the number of cells after one generation (41). x_P is the fraction of the population in the protein state P and $\lambda_{P,S}$ is the growth rate of cells in the protein state P and stress level S. The values of P correspond to the protein levels $\{0-100, 100-200, ..., 9900-10000\}$ molecules. Because the population stays in equilibrium, the total growth is

$$N_t/N_0 = \left(\sum_P x_P 2^{\lambda_{P,S}} \right)^t, \tag{2.10}$$

where t is the time spent in equilibrium conditions measured in generations. Note that the population grows if the value of the sum is greater than 1.

For the case with two environments, the ratio of final to initial cells is determined by

$$N_t/N_0 = \left(\sum_P x_P 2^{\lambda_{P,S_l}} \right)^{t_l} \cdot \left(\sum_P x_P 2^{\lambda_{P,S_h}} \right)^{t_h}, \tag{2.11}$$

where t_l and t_h are the times spent in low and high stress conditions. S_l and S_h are the low and high stress conditions. Instead of calculating the product of ratios, we record the logarithm of the products of ratios

$$\log\left(N_t/N_0\right) = t_l \log\left(\sum_P x_P 2^{\lambda_{P,S_l}}\right) + t_h \log\left(\sum_P x_P 2^{\lambda_{P,S_h}}\right). \tag{2.12}$$

As the fitness function in our evolutionary algorithm, we use

$$R = \frac{\log\left(N_t/N_0\right)}{t_l + t_h}, \tag{2.13}$$

which corresponds to the geometric growth rate. In the special case where no cells survive ($\lambda_{P,S_h} = -1$ for all values of P), we set R to -1. When some cells survive, R evaluates to a number between 0 and 1, where 0 indicates that the population is not growing at all and 1 indicates that it is growing optimally.

Evolutionary algorithm We used the Python differential evolution code (30), available online at `http://www1.icsi.berkeley.edu/~storn/code.html`. We modified it to use the Python module *numpy*, which allows for fast operations on vector objects. Differential evolution finds optimal or near-optimal solutions by iteratively improving a set of candidate solutions based on their fitness. For example, in the 2γ case, differential evolution evolves the six parameters a_1, b_1, w_1, a_2, b_2, and w_2.

Initialization of the population

The population was set to 40 trial vectors, following recommendations for good performance of the differential evolution algorithm from (42).

For the 1γ distribution, the initial population was set by creating vectors $\{a, b\}$ in the range $a = [0.5, 100]$, $b = [10, 400]$. For the full evolutionary algorithm, we used bounds $[0.5, 100]$ for a and $[10, 4000]$ for b to allow for parameters in the range of experimentally derived values from (28). The difference between the initialization ranges and bounds were empirically found to provide better convergence of the algorithm.

For the 2γ distribution, the initial population was created in the range $a_1 = [0.5, 2]$, $b_1 = [10, 400]$, $w_1 = [0, 1]$, $a_2 = [2, 100]$, $b_2 = [10, 400]$, and $w_2 = [0, 1]$; with bounds $a_1 = [0.5, 100]$, $b_1 = [10, 4000]$, $w_1 = [0, 10]$, $a_2 = [0.5, 100]$, $b_2 = [10, 4000]$, and $w_2 = [0, 10]$. The difference between the initialization ranges allows the two gamma distributions to start with proteins distributed between low and high protein expression levels to allow the evolution of bimodality.

For the case with no restriction on the protein distribution, we evolved the fraction of the population at each protein level, $p(P)$, directly with an initialization and bound range $[0, 1]$. The range has little effect on performance, since the final $p(P)$ values are normalized to $\sum_P p(P) = 1$. Given the large number of parameters, we initialized the population with 400 trial vectors, which we found to improve convergence.

Evolution and parameters

For each trial vector x_i in the population, a mutant vector v_i was created using the DE/rand/1/bin method (30), which combines three random trial vectors in the population, x_{r_1}, x_{r_2}, and x_{r_3}, according to

$$v_i = x_{r_1} + F \cdot (x_{r_2} - x_{r_3}), \tag{2.14}$$

where the multiplier F was chosen randomly from the range $[0.5, 2]$, since these values have been shown to improve convergence, especially when the fitness function is noisy (42).

If the population had not converged after 50 generations (see termination description below), the algorithm was switched from DE/rand/1/bin to DE/best/1/bin (30), and the mutant vector was created as

$$v_i = x_{best} + F \cdot (x_{r_1} - x_{r_2}), \tag{2.15}$$

where x_{best} is the trial vector with highest fitness in the population. This change in the method allows for a more refined search in the latter parts of the evolution.

The mutant vector v_i is combined with the i$^{\text{th}}$ trial vector, x_i, in the population using 90% of the values in v_i and 10% of the values in x_i, i.e. the crossover rate is 0.9, as suggested by Price and Storn in the case of parameter dependence (42). The resulting vector, u_i, substitutes x_i for the set of trial vectors if it allows for a higher fitness value than x_i.

Termination

The algorithm was allowed to run for 500 generations, or until convergence. Convergence was defined as being achieved if the difference between the mean fitness of the population and the fitness of all candidate solutions was within 10^{-10} fitness units.

Sensing case When the cells are able to sense the environment, they can adapt their distribution in high stress conditions. The switching rates between protein states are on the order of the doubling time. Thus, we assumed one generation is required to sense and adapt to the environment.

The log of the ratio of final to initial number of cells in this case is calculated as

$$\log\left(N_t/N_0\right) = t_l \log\left(\sum_P x_P 2^{\lambda_{P,S_l}}\right) + \log\left(\sum_P x_P 2^{\lambda_{P,S_h}}\right) + (t_h - 1)\log\left(\sum_P y_P 2^{\lambda_{P,S_h}}\right), \tag{2.16}$$

where x_P is the fraction of cells in protein level P adapted to the low stress environment and y_P is the fraction of cells adapted to the high stress environment. We obtained the distribution of y_P values by evolving the optimal unimodal distribution in fixed high stress conditions. The first term in this equation describes the population in low stress, the middle term describes the population during the one generation after the transition from low to high stress, and the final term describes the population during the time in high stress.

Addition of noise in the environment We created exponential distributions of noise with mean noise levels between 0.025 and 0.5mM. A random value from this distribution was added (subtracted) from the 0mM (10mM) environments. While the noise changes between evolutionary generations of the algorithm, the noise was identical for all vectors x_i, v_i and u_i (see "Evolutionary algorithm") within a generation. When the stress level is deterministic the fitness can be calculated after visiting the high and low stress conditions once (Eq. 2.12 or 2.16). For the case with noise, the stress level changes with time. To reduce the variation in highest obtainable fitness between generations, the growth rate was calculated after 100 alternative visits to low and high stress conditions. To further reduce the differences between the simulations in the 1γ and 2γ cases, three independent simulations were run, and the simulation with the highest fitness was recorded.

Intermediate environment An intermediate environment was added, with a stressor concentration of 1.1mM. We selected this value because the optimal concentration of protein in a fixed 1.1mM environment is half way between the optimal concentration for 0mM and 10mM due to the nonlinear nature of the growth rate function (Eq. 2.8). The fitness of a population with a distribution of protein levels was calculated by cycling between the three stress conditions in the order: low, medium, low, and high stress.

References

[1] Simons AM. Modes of response to environmental change and the elusive empirical evidence for bet hedging. Proceedings of the Royal Society B: Biological Sciences. 2011 Jun;278(1712):1601–9.

[2] Leibler S, Kussell E. Individual histories and selection in heterogeneous populations. Proceedings of the National Academy of Sciences. 2010 Jul;107(29):13183–8.

[3] Meyers LA, Bull JJ. Fighting change with change: adaptive variation in an uncertain world. Trends in Ecology & Evolution. 2002;5347(December):551–557.

[4] Keren I, Kaldalu N, Spoering A, Wang Y, Lewis K. Persister cells and tolerance to antimicrobials. FEMS Microbiology Letters. 2004 Jan;230(1):13–18.

[5] Fauvart M, De Groote VN, Michiels J. Role of persister cells in chronic infections: clinical relevance and perspectives on anti-persister therapies. Journal of Medical Microbiology. 2011;(60):699–709.

[6] Grossman AD. Genetic networks controlling the initiation of sporulation and the development of genetic competence in Bacillus subtilis. Annual Review of Genetics. 1995;29(1):477–508.

[7] Süel GM, Garcia-Ojalvo J, Liberman LM, Elowitz MB. An excitable gene regulatory circuit induces transient cellular differentiation. Nature. 2006 Mar;440(7083):545–50.

[8] Rainey PB, Beaumont HJE, Ferguson GC, Gallie J, Kost C, Libby E, et al. The evolutionary emergence of stochastic phenotype switching in bacteria. Microbial Cell Factories. 2011 Aug;10 Suppl 1:S14.

[9] Alekshun MN, Levy SB. Molecular Mechanisms of Antibacterial Multidrug Resistance; 2007.

[10] Wood KB, Cluzel P. Trade-offs between drug toxicity and benefit in the multi-antibiotic resistance system underlie optimal growth of E. coli. BMC Systems Biology. 2012 Jan;6(1):48.

[11] Balaban N, Merrin J, Chait R, Kowalik L, Leibler S. Bacterial persistence as a phenotypic switch. Science. 2004;305(September):1622–1625.

[12] Beaumont HJE, Gallie J, Kost C, Ferguson GC, Rainey PB. Experimental evolution of bet hedging. Nature. 2009 Nov;462(7269):90–3.

[13] Rainey PB, Travisano M. Adaptive radiation in a heterogeneous environment. Nature. 1998;394:69–72.

[14] Blake WJ, Balázsi G, Kohanski MA, Isaacs FJ, Murphy KF, Kuang Y, et al. Phenotypic consequences of promoter-mediated transcriptional noise. Molecular Cell. 2006;24(6):853–865.

[15] Zhuravel D, Fraser D, St-Pierre S, Tepliakova L, Pang WL, Hasty J, et al. Phenotypic impact of regulatory noise in cellular stress-response pathways. Systems and Synthetic Biology. 2010 Jun;4(2):105–16.

[16] Ito Y, Toyota H, Kaneko K, Yomo T. How selection affects phenotypic fluctuation. Molecular Systems Biology. 2009 Jan;5:264.

[17] Levins R. Evolution in Changing Environments: Some Theoretical Explorations. Princeton University Press. 1968;.

[18] Lachmann M, Jablonka E. The Inheritance of Phenotypes: an Adaptation to Fluctuating Environments. Journal of Theoretical Biology. 1996;(181):1–9.

[19] Thattai M, van Oudenaarden A. Stochastic gene expression in fluctuating environments. Genetics. 2004 May;167(1):523–30.

[20] Kussell E, Leibler S. Phenotypic diversity, population growth, and information in fluctuating environments. Science. 2005 Sep;309(5743):2075–8.

[21] Gander MJ, Mazza C, Rummler H. Stochastic gene expression in switching environments. Journal of Mathematical Biology. 2007 Aug;55(2):249–69.

[22] Gaál B, Pitchford JW, Wood AJ. Exact results for the evolution of stochastic switching in variable asymmetric environments. Genetics. 2010 Apr;184(4):1113–9.

[23] Visco P, Allen RJ, Majumdar SN, Evans MR. Switching and growth for microbial populations in catastrophic responsive environments. Biophysical Journal. 2010 Apr;98(7):1099–108.

[24] Müller J, Hense Ba, Fuchs TM, Utz M, Pötzsche C. Bet-hedging in stochastically switching environments. Journal of Theoretical Biology. 2013 Nov;336:144–57.

[25] Wolf DM, Vazirani VV, Arkin AP. Diversity in times of adversity: probabilistic strategies in microbial survival games. Journal of Theoretical Biology. 2005 May;234(2):227–53.

[26] Solopova A, van Gestel J, Weissing FJ, Bachmann H, Teusink B, Kok J, et al. Bet-hedging during bacterial diauxic shift. Proceedings of the National Academy of Sciences. 2014 May;111(20):7427–32.

[27] Acar M, Mettetal JT, van Oudenaarden A. Stochastic switching as a survival strategy in fluctuating environments. Nature Genetics. 2008 Apr;40(4):471–5.

[28] Taniguchi Y, Choi PJ, Li GW, Chen H, Babu M, Hearn J, et al. Quantifying E. coli proteome and transcriptome with single-molecule sensitivity in single cells. Science (New York, NY). 2010 Jul;329(5991):533–8.

[29] Smits WK, Kuipers OP, Veening JW. Phenotypic variation in bacteria: the role of feedback regulation. Nature reviews Microbiology. 2006 Apr;4(4):259–71.

[30] Storn R, Price K. Differential evolution–a simple and efficient heuristic for global optimization over continuous spaces. Journal of Global Optimization. 1997;11(4):341–359.

[31] Friedman N, Cai L, Xie X. Linking Stochastic Dynamics to Population Distribution: An Analytical Framework of Gene Expression. Physical Review Letters. 2006 Oct;97(16):168302.

[32] Salathé M, Van Cleve J, Feldman MW. Evolution of stochastic switching rates in asymmetric fitness landscapes. Genetics. 2009 Aug;182(4):1159–64.

[33] Rosenfeld N, Young JW, Alon U, Swain PS, Elowitz MB. Gene regulation at the single-cell level. Science. 2005 Mar;307(5717):1962–5.

[34] Charlebois DA, Kærn M. What all the noise is about: the physical basis of cellular individuality. Canadian Journal of Physics. 2012;923:919–923.

[35] Kaern M, Elston TC, Blake WJ, Collins JJ. Stochasticity in gene expression: from theories to phenotypes. Nature Reviews Genetics. 2005 Jun;6(6):451–64.

[36] Rotem E, Loinger A, Ronin I, Levin-Reisman I, Gabay C, Shoresh N, et al. Regulation of phenotypic variability by a threshold-based mechanism underlies bacterial persistence. Proceedings of the National Academy of Sciences. 2010 Jul;107(28):12541–6.

[37] Joers A, Kaldalu N, Tenson T. The frequency of persisters in Escherichia coli reflects the kinetics of awakening from dormancy. Journal of bBcteriology. 2010;192(13):3379–3384.

[38] Futcher B, Latter G, Monardo P, McLaughlin C, Garrels J. A sampling of the yeast proteome. Molecular and Cellular Biology. 1999;19(11):7357–7368.

[39] Garcia-Bernardo J, Dunlop MJ. Noise and low-level dynamics can coordinate multicomponent bet hedging mechanisms. Biophysical Journal. 2015;108(1):184–193.

[40] Dekel E, Alon U. Optimality and evolutionary tuning of the expression level of a protein. Nature. 2005;436(July):588–592.

[41] Monod J. The Growth of Bacterial Cultures. Annual Review of Microbiology. 1949;3:371–394.

[42] Price K, Storn RM, Lampinen JA. Differential evolution: a practical approach to global optimization. Springer Science & Business Media; 2006.

Chapter 3

Discussion

3.1 Discussion and Future Work

Taken together, our results have contributed to the further understanding of noise in biological systems. Noise in gene expression has been proposed as a bet-hedging mechanism (10). In this thesis, we sought to further define the conditions where noise is beneficial. We created a stochastic model to study the role of variability in a regulator controlling a suite of downstream genes. Our results show that noise in gene expression is able to coordinate multi-component stress response mechanisms, increasing the survival concentration of a stressor with no extra cost for the population. Furthermore, we used evolutionary algorithms to study how noise in gene expression – which produces unimodal distribution of proteins – compares to bimodality in an environment fluctuating between low and high stress conditions. We found that while bimodality is beneficial if the stress

states are well-defined, unimodal distributions are just as good when the environment is noisy or composed of many stress states.

Although our findings are computational, we were motivated by experimental result indicating that noise can coordinate multiple downstream genes. First, noise-driven quantitative correlations have been shown in *S. cerevisiae* in the expression of stress-response genes (60). Second, Hansen et al. (61) have studied the transmission of low-level fluctuations in *S. cerevisiae* stress response. They showed that two promoter classes exist: Promoters with fast dynamics are able to transmit low-level fluctuations in an upstream regulator, weakly expressing resistance genes. On the contrary, promoters with slow dynamics filter upstream low-level fluctuations. Nevertheless, careful examination of the experimental data for slow dynamics promoter reveals strong simultaneous expression of downstream genes in a small fraction of the population (Fig. 3.1). This is the case even in the presence of low-level upstream pulsing. A similar experiment could help quantify the correlation between downstream genes in the presence of a noisy upstream regulator. For this, two copies of a gene controlled by a regulator could be fused with different fluorescent proteins. Thus, the two downstream genes, and a regulator controlled by a noisy genetic network could be transformed into bacteria. To assess the correlation between the downstream genes, alternative regulators with different levels of noise could be constructed. The fluorescence of both downstream genes could then be measured simultaneously in thousands of cells using flow cytometry.

Similarly, microfluidics could be used to assess the benefit of bimodality. For this, we could transform bacteria with a gene conferring resistance to an antibiotic. Two populations of bacteria could then be transformed with plasmids containing the gene under the control of

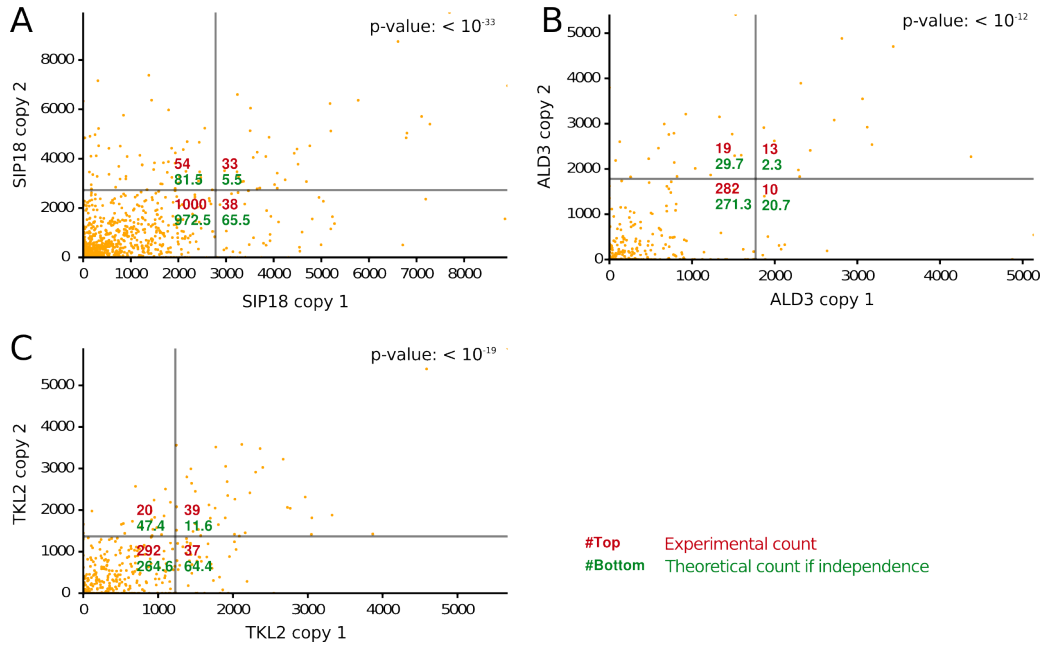

Figure 3.1: **Low-level pulsing coordinates downstream genes.** The data plotted in this figure is from Hansen et al. (2013). The expression (in AU) in a population of *S. cerevisiae* cells of two identical copies of the following MNS2 downstream genes is plotted: (A) SIP18, (B) ALD3 and (C) TKL2. Vertical and horizontal gray lines show $\frac{1}{3}$ of the 90^{th} percentile, dividing the plot into four quarters. The experimental number of cells in each quarter and the theoretical number of cells assuming independence between downstream genes are shown. Note that independence is expected if the promoter was able to filter the low-level dynamics. p-values are based on a Pearson's χ^2 test for independence. Data corresponds to one, 30 minute, 690 nM 1-NM-PP1 pulse. 1-NM-PP1 induces Mns2, but the induction time and concentration used produce a small pulse in Mns2, which is filtered at the population level for the genes displayed.

genetic networks, producing bistable and unimodal distribution of proteins. We could next use microfluidics for dynamic modification of the antibiotic concentration. The benefit of bimodality could be measured by quantifying the growth rate of the two constructs under different fluctuating environments.

Another limitation of our findings is our assumption that populations are in equilibrium. In the presence of a stress, the cells are assumed to be switching between phenotype states

maintaining a fixed distribution of protein levels. However, random fluctuations in gene expression can be maintained for up to three generations (62), and shorter half-lifes can be produced with degradation tags (63). In addition, bistable networks can maintain protein levels for even longer times (51). Therefore, the population can tune the switching rate between phenotypic states to increase growth rates (48). If the high stress conditions last for long periods of time, a bistable distribution of protein can be beneficial, since they allow for lower switching rates than unimodal distributions. Further computational and experimental research is needed to asses how growth rate is affected when the autocorrelation times in the protein levels are varied.

Our analysis has applications in many fields. In biocontrol, microorganisms are released to the environment to protect crops from pests (64). Understanding the stress types they may encounter during the process can allow for the design of more resilient agents. Similarly, the design of new probiotics can also benefit from more resilient microbes, that can displace pathogenic bacteria in the intestinal system (65). Finally, although we focus in microorganisms, our results are applicable to larger organisms, and thus can be applied to population ecology. For example, partial migration, where a subset of the population move temporally to another niche, has been found in birds, mammals, amphibians, fish and shrimp (66). Migration reduces intraspecies competition and allows for higher growth rates. However, the cost of migration includes increased predation and energetic costs. Therefore, partial migration may be seen as a bet-hedging strategy (67). Variability in animal behavior can also increase growth rates in the ever changing nature.

We conclude that noise can be a straightforward bet-hedging strategy. Noise in an upstream regulator can effectively coordinate multi-component stress response mechanisms in a small subset of the population, increasing the survivable concentration of a stressor without increasing metabolic cost. In addition, for mono-component stress response mechanisms under realistic environmental conditions with uncertainty in stress levels, noise in gene expression – corresponding to a unimodal distribution of protein levels – can provide the same balance of high growth and survival rates than a more complicated, bi-modal strategy. Our results bring insight into the mechanisms that microorganisms use to survive in uncertain environments, and provide us with a method to evaluate both the growth of microorganisms in a fluctuating environment, and the effect of drug administration profiles in population of cells.

Comprehensive Bibliography

[1] Carlet J, Collignon P, Goldmann D, Goossens H, Gyssens IC, Harbarth S, et al. Society's failure to protect a precious resource: antibiotics. The Lancet. 2011;378(9788):369–371.

[2] Harzevili FD, Chen H. Microbial Biotechnology: Progress and Trends. CRC Press; 2014.

[3] Le Dréan G, Mounier J, Vasseur V, Arzur D, Habrylo O, Barbier G. Quantification of Penicillium camemberti and P. roqueforti mycelium by real-time PCR to assess their growth dynamics during ripening cheese. International Journal of Food Microbiology. 2010;138(1):100–107.

[4] van de Guchte M, Serror P, Chervaux C, Smokvina T, Ehrlich SD, Maguin E. Stress responses in lactic acid bacteria. Antonie Van Leeuwenhoek. 2002;82(1-4):187–216.

[5] Alekshun MN, Levy SB. Molecular Mechanisms of Antibacterial Multidrug Resistance; 2007.

[6] Keren I, Kaldalu N, Spoering A, Wang Y, Lewis K. Persister cells and tolerance to antimicrobials. FEMS Microbiology Letters. 2004 Jan;230(1):13–18.

[7] Ni M, Decrulle AL, Fontaine F, Demarez A, Taddei F, Lindner AB. Pre-disposition and epigenetics govern variation in bacterial survival upon stress. PLoS Genetics. 2012;8(12):e1003148.

[8] Hecker M, Völker U. General stress response of Bacillus subtilis and other bacteria. Advances in Microbial Physiology. 2001;44:35–91.

[9] Wood KB, Cluzel P. Trade-offs between drug toxicity and benefit in the multi-antibiotic resistance system underlie optimal growth of E. coli. BMC Systems Biology. 2012 Jan;6(1):48.

[10] Fraser D, Kærn M. A chance at survival: gene expression noise and phenotypic diversification strategies. Molecular Microbiology. 2009;71(6):1333–1340.

[11] Blake WJ, Balázsi G, Kohanski MA, Isaacs FJ, Murphy KF, Kuang Y, et al. Phenotypic consequences of promoter-mediated transcriptional noise. Molecular Cell. 2006;24(6):853–865.

[12] Maheshri N, O'Shea EK. Living with noisy genes: how cells function reliably with inherent variability in gene expression. Annu Rev Biophys Biomol Struct. 2007;36:413–434.

[13] Grkovic S, Brown MH, Skurray RA. Regulation of bacterial drug export systems. Microbiology and Molecular Biology Reviews. 2002;66(4):671–701.

[14] Martin RG, Rosner JL. Transcriptional and translational regulation of the marRAB multiple antibiotic resistance operon in Escherichia coli. Molecular Microbiology. 2004;53(1):183–191.

[15] Vinué L, McMurry LM, Levy SB. The 216-bp marB gene of the marRAB operon in Escherichia coli encodes a periplasmic protein which reduces the transcription rate of marA. FEMS Microbiology Letters. 2013;345(1):49–55.

[16] Garcia-Bernardo J, Dunlop MJ. Tunable stochastic pulsing in the Escherichia coli multiple antibiotic resistance network from interlinked positive and negative feedback loops. PLoS Computational Biology. 2013 Jan;9(9):e1003229.

[17] Zhuravel D, Fraser D, St-Pierre S, Tepliakova L, Pang WL, Hasty J, et al. Phenotypic impact of regulatory noise in cellular stress-response pathways. Systems and Synthetic Biology. 2010 Jun;4(2):105–16.

[18] Luscombe NM, Babu MM, Yu H, Snyder M, Teichmann Sa, Gerstein M. Genomic analysis of regulatory network dynamics reveals large topological changes. Nature. 2004 Sep;431(7006):308–12.

[19] Dunlop MJ, Cox RS, Levine JH, Murray RM, Elowitz MB. Regulatory activity revealed by dynamic correlations in gene expression noise. Nature Genetics. 2008 Dec;40(12):1493–8.

[20] Garcia-Bernardo J, Dunlop MJ. Noise and low-level dynamics can coordinate multicomponent bet hedging mechanisms. Biophysical Journal. 2015;108(1):184–193.

[21] Stewart GR, Robertson BD, Young DB. Tuberculosis: a problem with persistence. Nature Reviews Microbiology. 2003;1(2):97–105.

[22] Veening JW, Smits W, Hamoen L, Kuipers O. Single cell analysis of gene expression patterns of competence development and initiation of sporulation in Bacillus subtilis grown on chemically defined media. Journal of Applied Microbiology. 2006;101(3):531–541.

[23] Salathé M, Van Cleve J, Feldman MW. Evolution of stochastic switching rates in asymmetric fitness landscapes. Genetics. 2009 Aug;182(4):1159–64.

[24] Müller J, Hense Ba, Fuchs TM, Utz M, Pötzsche C. Bet-hedging in stochastically switching environments. Journal of Theoretical Biology. 2013 Nov;336:144–57.

[25] Lachmann M, Jablonka E. The Inheritance of Phenotypes: an Adaptation to Fluctuating Environments. Journal of Theoretical Biology. 1996;(181):1–9.

[26] Levins R. Evolution in Changing Environments: Some Theoretical Explorations. Princeton University Press. 1968;.

[27] Kussell E, Leibler S. Phenotypic diversity, population growth, and information in fluctuating environments. Science. 2005 Sep;309(5743):2075–8.

[28] Donaldson-Matasci MC, Bergstrom CT, Lachmann M. The fitness value of information. Oikos. 2010 Feb;119(2):219–230.

[29] Solopova A, van Gestel J, Weissing FJ, Bachmann H, Teusink B, Kok J, et al. Bet-hedging during bacterial diauxic shift. Proceedings of the National Academy of Sciences. 2014 May;111(20):7427–32.

[30] Taniguchi Y, Choi PJ, Li GW, Chen H, Babu M, Hearn J, et al. Quantifying E. coli proteome and transcriptome with single-molecule sensitivity in single cells. Science (New York, NY). 2010 Jul;329(5991):533–8.

[31] Friedman N, Cai L, Xie X. Linking Stochastic Dynamics to Population Distribution: An Analytical Framework of Gene Expression. Physical Review Letters. 2006 Oct;97(16):168302.

[32] Simons AM. Modes of response to environmental change and the elusive empirical evidence for bet hedging. Proceedings of the Royal Society B: Biological Sciences. 2011 Jun;278(1712):1601–9.

[33] Leibler S, Kussell E. Individual histories and selection in heterogeneous populations. Proceedings of the National Academy of Sciences. 2010 Jul;107(29):13183–8.

[34] Meyers LA, Bull JJ. Fighting change with change: adaptive variation in an uncertain world. Trends in Ecology & Evolution. 2002;5347(December):551–557.

[35] Fauvart M, De Groote VN, Michiels J. Role of persister cells in chronic infections: clinical relevance and perspectives on anti-persister therapies. Journal of Medical Microbiology. 2011;(60):699–709.

[36] Grossman AD. Genetic networks controlling the initiation of sporulation and the development of genetic competence in Bacillus subtilis. Annual Review of Genetics. 1995;29(1):477–508.

[37] Süel GM, Garcia-Ojalvo J, Liberman LM, Elowitz MB. An excitable gene regulatory circuit induces transient cellular differentiation. Nature. 2006 Mar;440(7083):545–50.

[38] Rainey PB, Beaumont HJE, Ferguson GC, Gallie J, Kost C, Libby E, et al. The evolutionary emergence of stochastic phenotype switching in bacteria. Microbial Cell Factories. 2011 Aug;10 Suppl 1:S14.

[39] Balaban N, Merrin J, Chait R, Kowalik L, Leibler S. Bacterial persistence as a phenotypic switch. Science. 2004;305(September):1622–1625.

[40] Beaumont HJE, Gallie J, Kost C, Ferguson GC, Rainey PB. Experimental evolution of bet hedging. Nature. 2009 Nov;462(7269):90–3.

[41] Rainey PB, Travisano M. Adaptive radiation in a heterogeneous environment. Nature. 1998;394:69–72.

[42] Ito Y, Toyota H, Kaneko K, Yomo T. How selection affects phenotypic fluctuation. Molecular Systems Biology. 2009 Jan;5:264.

[43] Thattai M, van Oudenaarden A. Stochastic gene expression in fluctuating environments. Genetics. 2004 May;167(1):523–30.

[44] Gander MJ, Mazza C, Rummler H. Stochastic gene expression in switching environments. Journal of Mathematical Biology. 2007 Aug;55(2):249–69.

[45] Gaál B, Pitchford JW, Wood AJ. Exact results for the evolution of stochastic switching in variable asymmetric environments. Genetics. 2010 Apr;184(4):1113–9.

[46] Visco P, Allen RJ, Majumdar SN, Evans MR. Switching and growth for microbial populations in catastrophic responsive environments. Biophysical Journal. 2010 Apr;98(7):1099–108.

[47] Wolf DM, Vazirani VV, Arkin AP. Diversity in times of adversity: probabilistic strategies in microbial survival games. Journal of Theoretical Biology. 2005 May;234(2):227–53.

[48] Acar M, Mettetal JT, van Oudenaarden A. Stochastic switching as a survival strategy in fluctuating environments. Nature Genetics. 2008 Apr;40(4):471–5.

[49] Smits WK, Kuipers OP, Veening JW. Phenotypic variation in bacteria: the role of feedback regulation. Nature reviews Microbiology. 2006 Apr;4(4):259–71.

[50] Storn R, Price K. Differential evolution–a simple and efficient heuristic for global optimization over continuous spaces. Journal of Global Optimization. 1997;11(4):341–359.

[51] Rosenfeld N, Young JW, Alon U, Swain PS, Elowitz MB. Gene regulation at the single-cell level. Science. 2005 Mar;307(5717):1962–5.

[52] Charlebois DA, Kærn M. What all the noise is about: the physical basis of cellular individuality. Canadian Journal of Physics. 2012;923:919–923.

[53] Kaern M, Elston TC, Blake WJ, Collins JJ. Stochasticity in gene expression: from theories to phenotypes. Nature Reviews Genetics. 2005 Jun;6(6):451–64.

[54] Rotem E, Loinger A, Ronin I, Levin-Reisman I, Gabay C, Shoresh N, et al. Regulation of phenotypic variability by a threshold-based mechanism underlies bacterial persistence. Proceedings of the National Academy of Sciences. 2010 Jul;107(28):12541–6.

[55] Joers A, Kaldalu N, Tenson T. The frequency of persisters in Escherichia coli reflects the kinetics of awakening from dormancy. Journal of bBcteriology. 2010;192(13):3379–3384.

[56] Futcher B, Latter G, Monardo P, McLaughlin C, Garrels J. A sampling of the yeast proteome. Molecular and Cellular Biology. 1999;19(11):7357–7368.

[57] Dekel E, Alon U. Optimality and evolutionary tuning of the expression level of a protein. Nature. 2005;436(July):588–592.

[58] Monod J. The Growth of Bacterial Cultures. Annual Review of Microbiology. 1949;3:371–394.

[59] Price K, Storn RM, Lampinen JA. Differential evolution: a practical approach to global optimization. Springer Science & Business Media; 2006.

[60] Stewart-Ornstein J, Weissman JS, El-Samad H. Cellular noise regulons underlie fluctuations in Saccharomyces cerevisiae. Molecular Cell. 2012 Feb;45(4):483–93.

[61] Hansen AS, O'Shea EK. Promoter decoding of transcription factor dynamics involves a trade-off between noise and control of gene expression. Molecular Systems Biology. 2013 Jan;9(704):704.

[62] Cocaign-Bousquet M, Even S, Lindley ND, Loubière P. Anaerobic sugar catabolism in Lactococcus lactis: genetic regulation and enzyme control over pathway flux. Applied Microbiology and Biotechnology. 2002;60(1-2):24–32.

[63] Belle A, Tanay A, Bitincka L, Shamir R, O'Shea EK. Quantification of protein half-lives in the budding yeast proteome. Proceedings of the National Academy of Sciences. 2006;103(35):13004–13009.

[64] Compant S, Duffy B, Nowak J, Clément C, Barka EA. Use of plant growth-promoting bacteria for biocontrol of plant diseases: principles, mechanisms of action, and future prospects. Applied and Environmental Microbiology. 2005;71(9):4951–4959.

[65] Kalliomäki M, Salminen S, Arvilommi H, Kero P, Koskinen P, Isolauri E. Probiotics in primary prevention of atopic disease: a randomised placebo-controlled trial. The Lancet. 2001;357(9262):1076–1079.

[66] Ogonowski M, Duberg J, Hansson S, Gorokhova E. Behavioral, ecological and genetic differentiation in an open environment–a study of a mysid population in the Baltic Sea. PloS one. 2013 Jan;8(3):e57210.

[67] Shaw AK, Levin SA. To breed or not to breed: a model of partial migration. Oikos. 2011;120(12):1871–1879.

[68] Reshes G, Vanounou S, Fishov I, Feingold M. Timing the start of division in E. coli: a single-cell study. Physical Biology. 2008;5(4):046001.

Appendix A: Supporting Information

A.1 Noise and Low-Level Dynamics Can Coordinate Multicomponent Bet-Hedging Mechanisms

APPENDIX A. SUPPORTING INFORMATION

SUPPLEMENTARY INFORMATION

Noise and Low-Level Dynamics Can Coordinate Multicomponent Bet Hedging Mechanisms

Javier Garcia-Bernardo[1], *Mary J. Dunlop*[2,*]
[1] *Department of Computer Science, University of Vermont, Burlington, VT, USA 05405*
[2] *School of Engineering, University of Vermont, Burlington, VT, USA 05405*
[*] *mjdunlop@uvm.edu*

APPENDIX A. SUPPORTING INFORMATION

SUPPLEMENTARY FIGURES

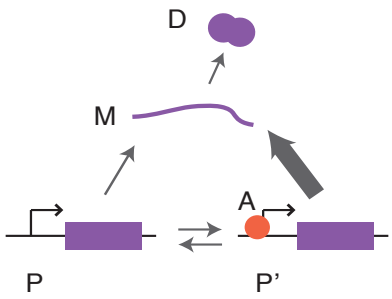

Figure S1. Schematic of the chemical reactions in the model. A, activator; P, unbound promoter; P', bound promoter; M, mRNA; D, downstream gene. Reactions and their rates are listed in Table S1.

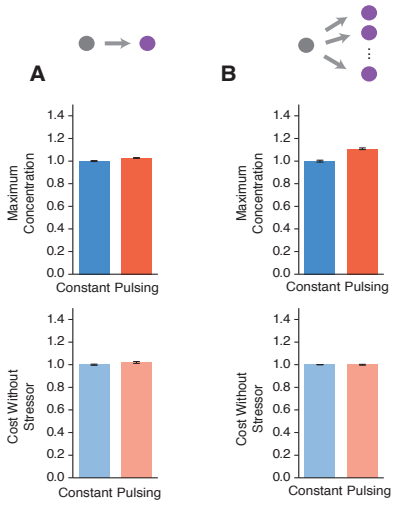

Figure S2. Linear cost function. The maximum concentration of stressor that 0.1% of cells in a population can survive and the corresponding average cost of growing in the absence of stressor. Values were measured for constant and pulsing activator dynamics for (A) one downstream gene and (B) ten downstream genes with K_D = 10,000 molecules. The cost function is linear (Methods). Error bars show standard deviations over three simulations.

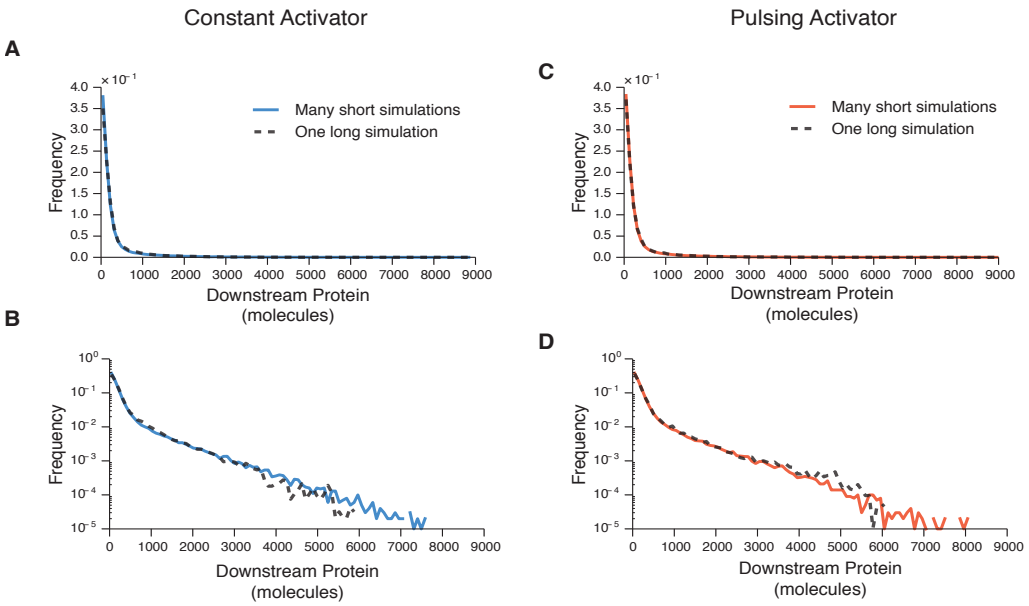

Figure S3. Histogram of downstream protein levels are equivalent when comparing data generated using a single 10^5 minute simulation (dashed line) and the final data points from 10^5 independent simulations (solid line). (A-B) Constant input distributions of downstream proteins plotted on (A) linear and (B) log scales. (C-D) Pulsing input distributions on (C) linear and (D) log scales.

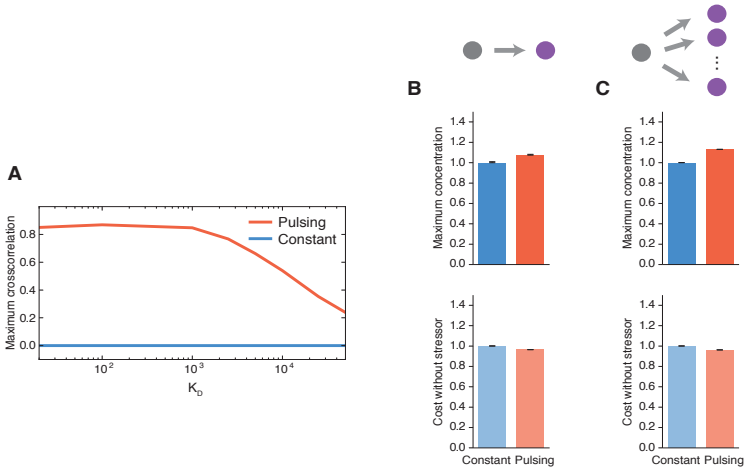

Figure S4. Fast promoter dynamics. (A) Maximum cross correlation as a function of the dissociation constant, K_D. (B, C) Maximum survivable concentration of stressor and the corresponding average cost of growing in the absence of stressor for constant and pulsing activator dynamics with (B) one downstream gene and (C) ten downstream genes with K_D = 10,000 molecules. Values from the pulsing dynamics are normalized to the constant input case. Error bars show standard deviations over three simulations.

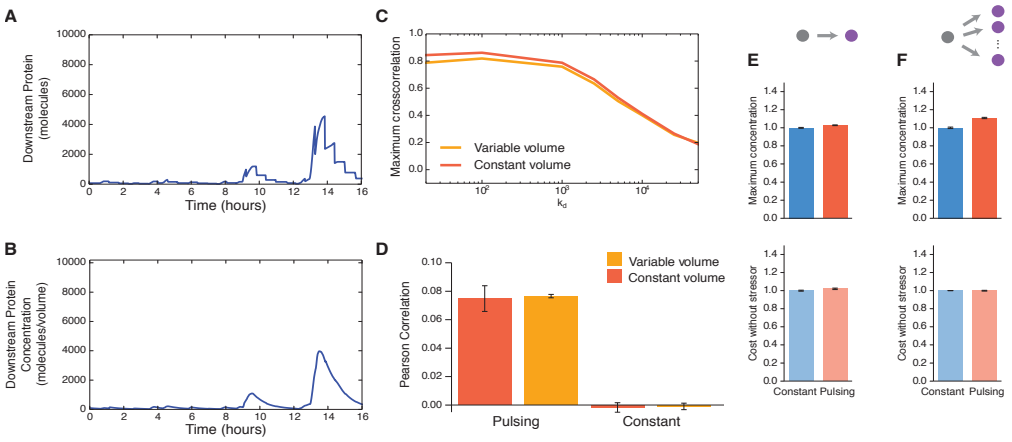

Figure S5. Effect of growth and partitioning on coordination. (A) Simulation with cell growth and partitioning showing the number of molecules of a downstream genes controlled by a pulsing input; K_D = 10,000 molecules. (B) Concentration of the downstream protein. In this plot the data from (A) is divided by the cell volume, which changes with time. (C) Maximum cross correlation between a pulsing activator and downstream protein as a function of K_D. The data generated using the model with cell division is similar to that without division and growth modeled explicitly, especially for large K_D values. (D) Pearson correlation between two downstream genes with K_D = 10,000 under the control of a pulsing input with and without growth and partitioning. (E, F) The maximum concentration of stressor that 0.1% of cells in a population can survive and the corresponding average cost of growing in the absence of stressor, when the effect of growth and partitioning are included. Values were measured for constant and pulsing activator dynamics for (E) one downstream gene and (F) ten downstream genes with K_D = 10,000 molecules. Error bars show standard deviations over three simulations.

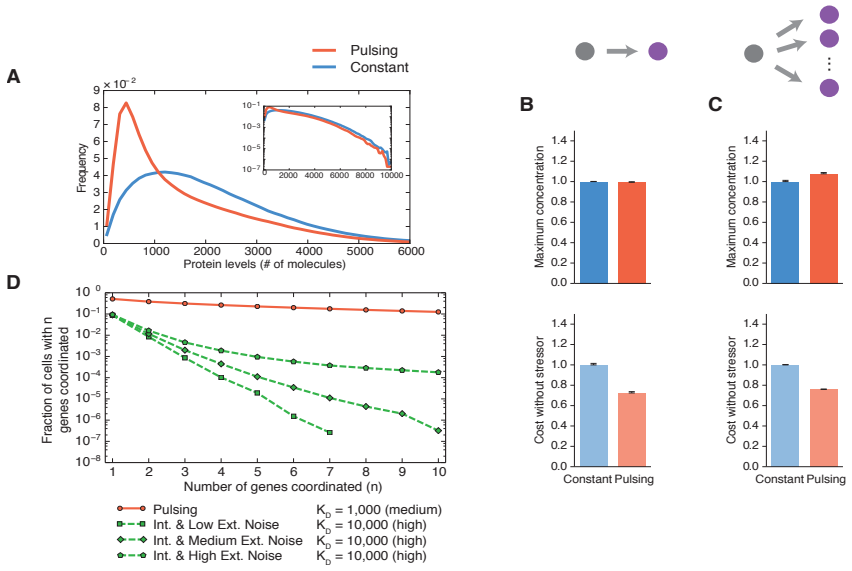

Figure S6. Medium dissociation constant (K_D = 1000 molecules). (A) Histograms of downstream gene expression. Inset shows the same data on a semilogarithmic scale. Note that the distributions are not identical due to the nonlinear nature of the activator curve: the pulsatile input spends more time at low values on the activation curve than the constant input does, resulting in lower mean expression of the downstream gene. (B, C) Maximum survivable concentration of stressor and the corresponding average cost of growing in the absence of stressor for constant and pulsing activator dynamics with (B) one downstream gene and (C) ten downstream genes with K_D = 1000 molecules. Values from the pulsing dynamics are normalized to the constant input case. Error bars show standard deviations over three simulations. (D) The fraction of cells with all downstream genes coordinated as a function of the number of downstream genes, *n*. The three noise data cases are reproduced from Fig. 4 for context and show results for infrequently activated downstream genes (K_D = 10,000 molecules). The pulsing data is for downstream genes with a medium dissociation constant (K_D = 1000 molecules). The plots do not start at the same point when *n* = 1 because the probability that a medium K_D gene is above the threshold for survival is greater than the probability that a high K_D gene is above the same threshold.

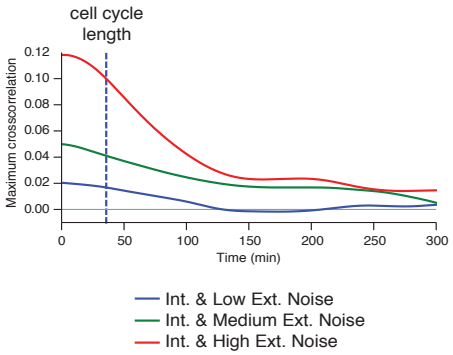

Figure S7. Cross correlation between two downstream genes (K_D = 10,000 molecules) with a noisy activator input. The three noise levels correspond to those shown in Fig. 3E and F.

APPENDIX A. SUPPORTING INFORMATION

SUPPLEMENTARY TEXT

Probability of coordination from dynamic and constant inputs

To gain further insight into the effects of coordination, we calculated the probabilities of coordinating *n* downstream genes using a simplified system, comparing a constant input with a simple dynamic input modeled by a square wave signal.

$$A_{constant} = X$$

$$A_{dynamic} \begin{cases} X\dfrac{T_{ON} + T_{OFF}}{T_{ON}}, & 0 < t \leq T_{ON} \\ 0, & T_{ON} < t \leq T_{OFF} \end{cases}$$

Note that, by construction, the two signals have the same mean. We assumed that the probability of turning on expression of a downstream gene is linearly related to the input, such that higher inputs result in an increased probability of activating the downstream gene. We found this to be a reasonable assumption based on empirical fits to our data (Supplementary Methods). The probability of coordinating *n* genes is the probability that all downstream genes are coordinated simultaneously

$$p(n) = (\gamma A)^n$$

Comparing the two types of inputs, we find

$$p_{constant}(n) = (\gamma X)^n$$

$$p_{dynamic}(n) = \frac{T_{ON}}{T_{ON} + T_{OFF}}(\gamma X \frac{T_{ON} + T_{OFF}}{T_{ON}})^n + \frac{T_{OFF}}{T_{ON} + T_{OFF}}(\gamma X\ 0)^n$$

$$= \left(\frac{T_{ON} + T_{OFF}}{T_{ON}}\right)^{n-1} (\gamma X)^n$$

The ratio of the two probabilities is

$$\frac{p_{dynamic}(n)}{p_{constant}(n)} = \left(\frac{T_{ON} + T_{OFF}}{T_{ON}}\right)^{n-1}$$

Therefore, the probability of coordinating *n* genes is always higher with pulsing than with a constant inputs when $n > 1$

$$p_{dynamic}(n) > p_{constant}(n)$$

Note that the two probabilities are equal when $n = 1$, as expected since coordination requires more than one gene.

SUPPLEMENTARY METHODS

Fast dynamics and moderate affinity downstream gene

Fast dynamics (Fig. S4) were modeled by increasing K_{ON} and K_{OFF}, as listed in Table S1, by a factor of 10. Note that the dissociation constant K_D ($=K_{OFF}/K_{ON}$) stays the same.

For the moderate affinity downstream gene (Fig. S6) K_D = 1000 molecules.

Coordination of *n* downstream genes
In the probability calculations described above we assumed a linear relationship between the probability of turning on expression of a downstream gene and the concentration of the activator. We determined the linear relationship empirically, finding $\gamma = 3.85 \times 10^{-4}$, by using Eureqa (1). This relationship holds for the thresholds described above with $R^2 > 0.99$ for the linear regression fit.

Modeling growth and partitioning
We assumed a cell division time of 34.7 minutes (equal to –ln(2)/0.02, the protein degradation half-life from Table S1). During growth, cellular volume increased following $V(t) = V_0\, 2^{t/34.7}$, where t is the time from the previous cell division event and V_0 was set to ln(2) to allow for a mean volume of 1. At every cell division event, cellular volume was reset to V_0 and the contents of the cell, including all protein, mRNA, and DNA species were partitioned between two daughter cells following a negative binomial distribution with probability 0.5. This distribution measures the number of molecules that are partitioned between each cell, assuming that every molecule is independent and has equal probability of being transmitted to each daughter cell. With variable volume, the units of K_{OFF} (Table S1) become V_r/min^{-1}, where V_r is the normalized volume, or volume/average volume. The pulsing signal was adjusted to match the dynamics of the case with fixed volume. To achieve this, at every time step the number of molecules of the activator was divided by the normalized volume. However, instead of multiplying K_{OFF} by V_r and dividing the number of molecules by V_r, K_{OFF} was held constant during the simulation and the number of molecules of the activator was varied according to the pulsing signal, and not corrected by volume.

Equivalence of long time simulation and many short time simulations
We verified that distributions of downstream protein levels generated using long simulations are equivalent to those generated by running many shorter simulations. This approach reduces the computation time required to generate data. For the long time course simulations in Fig. S3, we first performed an initialization simulation of 1440 minutes (24 hours) and used the final values from these data to set initial conditions. We then ran 10^5 minute simulations. For the short time simulations (Fig. S3), we used the initialization step and ran 10^5 simulations of 1440 minutes each, where the input activator signal had a random phase drawn from a uniform distribution between 0 and 240 minutes (corresponding to the period of the signal) to avoid sampling at the same point in the cycle every time.

Table S1. Reaction rates

Reaction rate	Value	Reaction	Comments

APPENDIX A. SUPPORTING INFORMATION

K_D	10,000 molecules		We set the amplitude of the pulses one order of magnitude lower than the K_D. One order of magnitude between the K_D of regulated genes has been observed experimentally (2, 3).
K_{OFF}	0.1 min^{-1}	$P' \rightarrow P + A$	Selected based on studies from both yeast and bacteria (3-5).
K_{ON}	K_{OFF}/K_D (molecules $min)^{-1}$	$P + A \rightarrow P'$	
α	0.02 min^{-1}	$P \rightarrow P + M$	Basal expression
α'	2 min^{-1}	$P' \rightarrow P' + M$	One order of magnitude higher than typical transcription rates in both in yeast (6) and *E. coli* (7). Note that these rates are based on only one RNA polymerase molecule, and several molecules work at the same time, therefore we increased the rate by an order of magnitude. The results are not sensitive to the exact value of α'.
λ_M	0.1 min^{-1}	$M \rightarrow \emptyset$	Typical degradation rate in *E. coli* (8) and in the feasible range for yeast (9).
β	10 min^{-1}		One order of magnitude higher than typical translation rates in *E. coli* (10), yeast (11), and mice (12). Note that these results are based on only one ribosome complex per mRNA, and several can work at the same time; the typical lag between translation initiation is 15 seconds in *E. coli* (13). The results are not sensitive to the exact value of β.
λ_D	0.02 min^{-1}		We used a typical half-life of 34.7 min, which corresponds with a stable protein in *E. coli* or a moderately degraded protein in yeast (14, 15).

Table S2. K_{ON} and noise contributions for different activator profiles. The K_{ON} value from Table S1 is multiplied by the constants listed here. $\eta_{tot}^2 = \eta_{int}^2 + \eta_{ext}^2$

Activator profile	**K_{ON} scaling factor**	**Total Noise (η_{tot})**	**Intrinsic Noise (η_{int})**	**Extrinsic Noise (η_{ext})**
Constant expression	1	0	0	0
Only Intrinsic Noise	1	0.21	0.21	0
Intrinsic & Low Extrinsic Noise	1.052	0.24	0.21	0.11

APPENDIX A. SUPPORTING INFORMATION

Intrinsic & Medium Extrinsic Noise	1.266	0.29	0.21	0.20
Intrinsic & High Extrinsic Noise	1.626	0.34	0.21	0.27

APPENDIX A. SUPPORTING INFORMATION

REFERENCES

1. Schmidt, M., and H. Lipson. 2013. Eureqa (Version 0.98 beta) [Software]. Available from http://www.eureqa.com/.
2. Lee, P., B.-R. Cho, H.-S. Joo, and J.-S. Hahn. 2008. Yeast Yak1 kinase, a bridge between PKA and stress-responsive transcription factors, Hsf1 and Msn2/Msn4. Molecular microbiology 70:882-895.
3. Hansen, A. S., and E. K. O'Shea. 2013. Promoter decoding of transcription factor dynamics involves a trade-off between noise and control of gene expression. Molecular systems biology 9:704.
4. So, L.-H., A. Ghosh, C. Zong, L. a. Sepúlveda, R. Segev, and I. Golding. 2011. General properties of transcriptional time series in Escherichia coli. Nature genetics 43:554-560.
5. China, A., P. Tare, and V. Nagaraja. 2010. Comparison of promoter-specific events during transcription initiation in mycobacteria. Microbiology (Reading, England) 156:1942-1952.
6. Pelechano, V., S. Chávez, and J. Pérez-Ortín. 2010. A complete set of nascent transcription rates for yeast genes. PLoS One 5.
7. Davenport, R. J., G. J. L. Wuite, R. Landick, and C. Bustamante. 2000. Single-Molecule Study of Transcriptional Pausing and Arrest by. Science 287:2497-2500.
8. Selinger, D. W., R. M. Saxena, K. J. Cheung, G. M. Church, and C. Rosenow. 2003. Global RNA Half-Life Analysis in Escherichia coli Reveals Positional Patterns of Transcript Degradation. Genome research 13:216-223.
9. Wang, Y., C. L. Liu, J. D. Storey, R. J. Tibshirani, D. Herschlag, and P. O. Brown. 2002. Precision and functional specificity in mRNA decay. Proceedings of the National Academy of Sciences of the United States of America 99:5860-5865.
10. Sørensen, M., C. Kurland, and S. Pedersen. 1989. Codon usage determines translation rate in Escherichia coli. Journal of molecular biology 207:365-377.
11. Bonven, B., and K. Gulløv. 1979. Peptide chain elongation rate and ribosomal activity in Saccharomyces cerevisiae as a function of the growth rate. Molecular and General Genetics 170:225-230.
12. Schwanhäusser, B., D. Busse, N. Li, G. Dittmar, J. Schuchhardt, J. Wolf, W. Chen, and M. Selbach. 2011. Global quantification of mammalian gene expression control. Nature 473:337-342.
13. Siwiak, M., and P. Zielenkiewicz. 2013. Transimulation - protein biosynthesis web service. PLoS One 8:e73943.
14. Belle, A., A. Tanay, L. Bitincka, R. Shamir, and E. K. O'Shea. 2006. Quantification of protein half-lives in the budding yeast proteome. Proceedings of the National Academy of Sciences of the United States of America 103:13004-13009.
15. Woldringh, C. L., M. a. de Jong, W. van den Berg, and L. Koppes. 1977. Morphological analysis of the division cycle of two Escherichia coli substrains during slow growth. Journal of bacteriology 131:270-279.

Appendix B: Supporting Information

B.1 Phenotypic diversity using bimodal and unimodal expression of stress response proteins in fluctuating environments

Supporting Information

Methods and additional information.

Fitness function After a transition time, and while the environment is constant, the distribution of protein states in a population is at equilibrium (1, 2). The equilibrium depends on the growth rates $\lambda_{P,S}$ and the switching rates between protein states (2). Here, we evolve the distribution of protein levels in the population that yields the highest growth rate. Therefore, we indirectly evolve the switching rates that produce that equilibrium. Furthermore, we assumed that the switching rates were on the order of the doubling time of a cell, which produces fast transition times, consistent with memory observed in the

level of proteins *in vivo* (3, 4). One concern is that the distribution of protein levels may change during the time in high stress, i.e. fewer cells may leave the resistant state than were leaving before the stress appeared. However, this effect is only pronounced when the switching rates are low compared with the differences in growth rates between cells (2). For our simulations, the maximum difference in growth rates is one order of magnitude below the doubling time of the cell, and therefore we assumed that the fraction of cells that leave the resistant state is constant through the different environmental conditions.

Differences in growth rates and relationship to time for one population to overtake another Provided the population is growing, the growth rate is normalized to be between $0-1$, where the value 1 corresponds to one cell division in the fastest possible cell division time.

The growth of cells is given by the equation

$$N_t = N_0 2^{R \cdot t},$$

where N_t is the final number of cells, N_0 is the initial number of cells, t is time that the population has been growing, and R is the growth rate.

The benefit of sensing or bimodality is measured in points, as the difference in growth rate multiplied by 100, with units (generations)$^{-1}$. For example, the ratio of cells between two populations 1 point apart is given by

$$\frac{2^{(x+0.01)t}}{2^{(x)t}} = 2^{0.01 \cdot t}.$$

Therefore, the time until the more fit condition represents 90% of the population (in other words, the ratio of more to less fit cells is 90:10, or 9) corresponds to

$$\begin{aligned} 9 &= 2^{0.01 \cdot t} \\ \log_2(9) &= 0.01 \cdot t \\ t &= 317 \text{ generations.} \end{aligned}$$

For *E. coli*, a generation corresponds to about 38 minutes in rich media (5), and therefore 317 generations is 8.4 days.

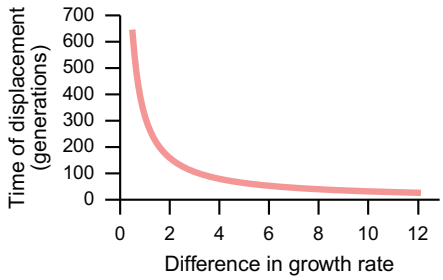

Figure B.1: **Relationship between difference in growth rate and time for population displacement.** The time required for a fast growing population to displace a slow growing one is plotted as a function of the difference in growth rate between the two populations. Displacement is defined as achieved when the more fit condition represents 90% of the population. See Supporting Text for additional discussion.

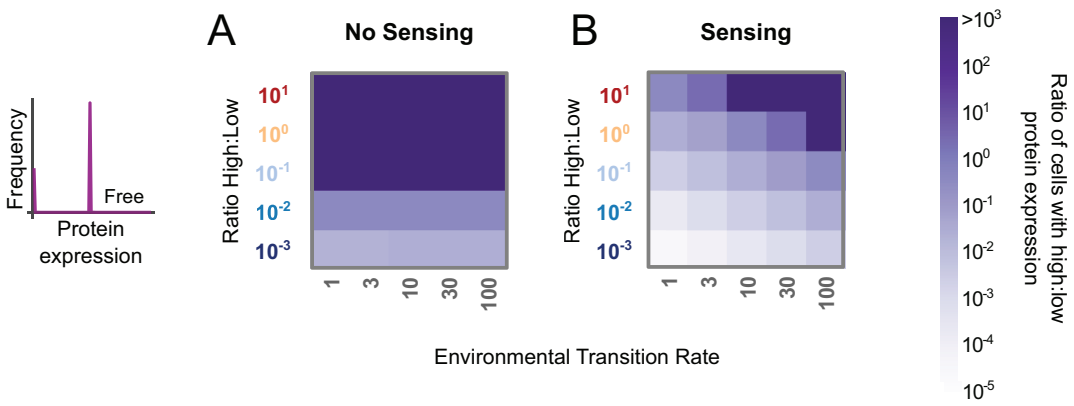

Figure B.2: **Bimodality is evolved in many conditions, even when there are no restrictions on the shape of the protein distribution.** The distribution of proteins is allowed to evolve freely, with no restrictions on its shape. Examples of the solutions are shown in the cartoon on the left. (A, B) The ratio of cells with high protein expression is plotted as a function of the environmental conditions for the (A) no sensing and (B) sensing case. Unimodal (dark purple) and bimodal (light purple) distributions are evolved.

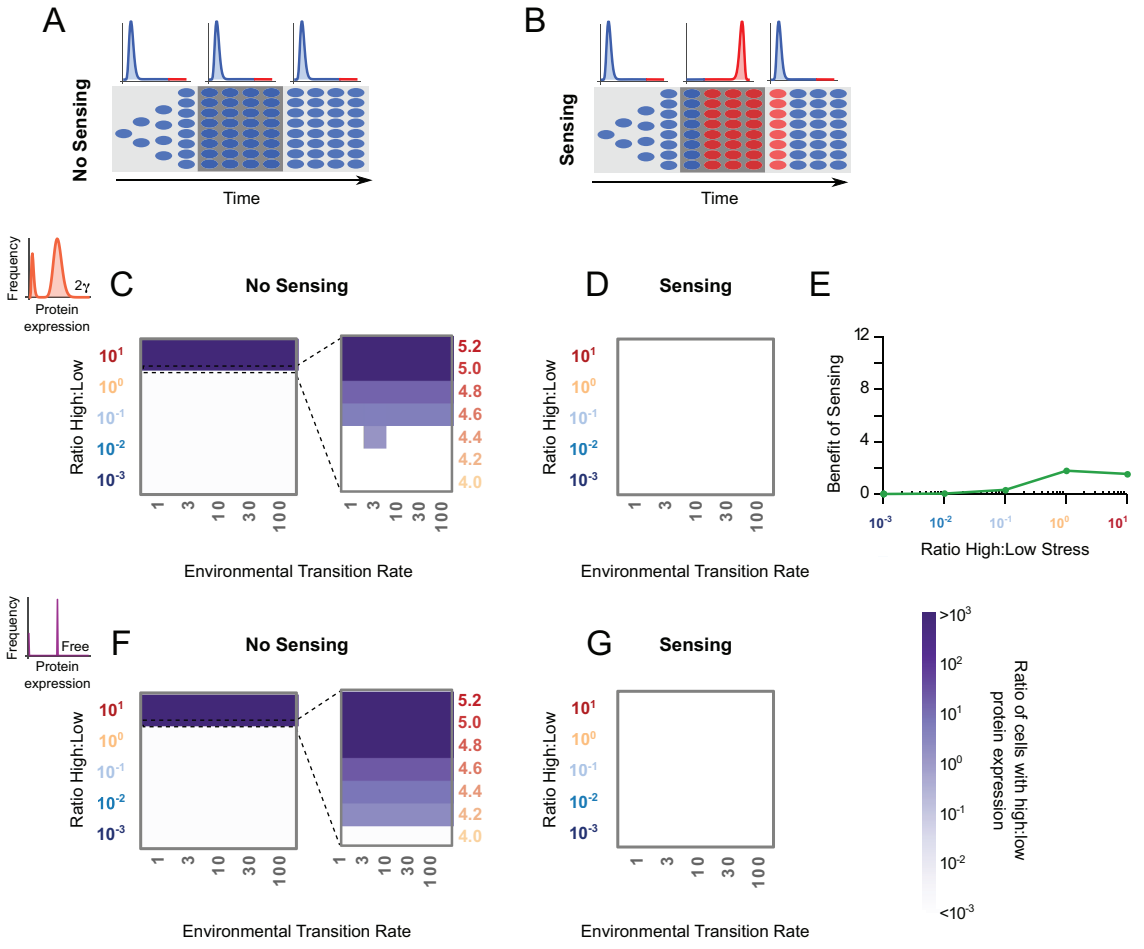

Figure B.3: **Bimodality is not generally evolved under weak stressors.** (A) Environments vary between low and high stress. Without sensing, the population can be composed of cells with low levels of protein expression (histograms). Under low stress, the population grows well. Under high stress, it stays latent. (B) With sensing, all populations sense and adapt to the current environment after one generation. (C–D) Simulations use the 2γ restriction. Ratio of cells with high to low protein expression for (C) no sensing and (D) sensing populations. Dark purple colors indicate unimodal distributions with high protein expression. Light purple is bimodal. White is a unimodal distribution with low protein expression. Inset shows the very small region where bimodality is evolved. (E) The benefit of sensing is plotted as a function of the ratio of high to low stress, reaching its maximum with symmetric environments. The benefit is measured as the difference in growth rate between the sensing and no sensing populations (Supporting Text). These simulations use an environmental transition rate of 10. Corresponding plots to (C–D) are shown in (F-G) for the case with no restrictions when evolving the protein distribution.

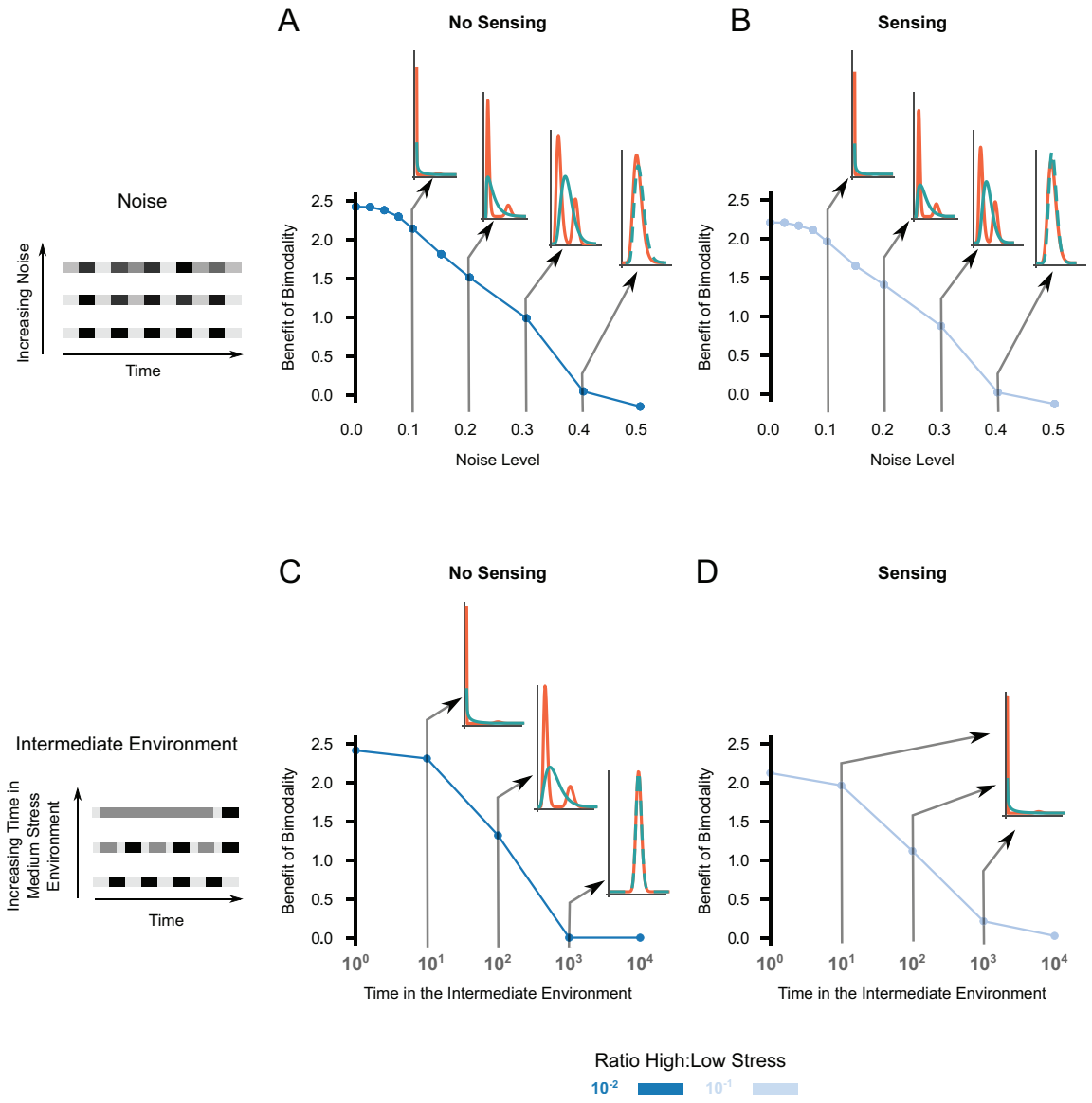

Figure B.4: **The benefit of bimodality decreases as noise or time in the intermediate environment is increased.** Examples of the distributions evolved with the 1γ and 2γ restrictions are shown (histograms) for increasing levels of noise in the (A) no sensing and (B) sensing cases. (C, D) The distributions evolved with the 1γ and 2γ cases are shown for increasing time in the intermediate, medium stress environment for the (C) no sensing and (D) sensing cases. For the sensing case, the evolved distributions are identical for all intermediate environment times, but the benefit decreases as the time spent in the intermediate environment becomes a larger fraction of the whole simulation time.

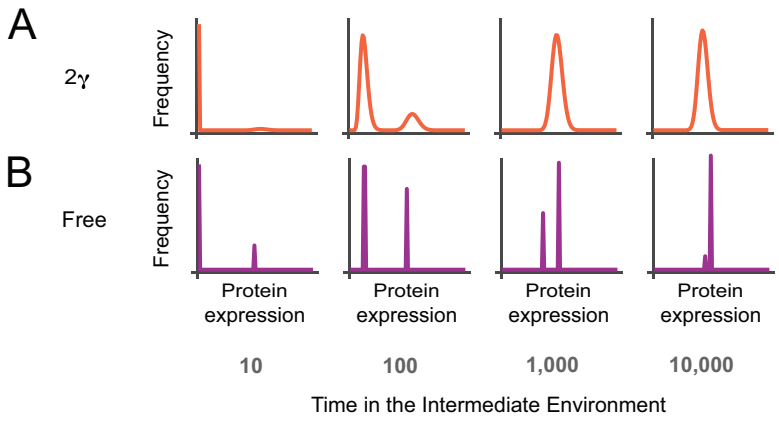

Figure B.5: **Bimodality, not trimodality, is evolved in the environment with three stress levels (low, medium, and high).** The distribution of protein levels is plotted for solutions obtained using the (A) 2γ requirement and (B) the case with no restrictions on protein distribution shape. For all simulations, the time in high and low stress is 10 generations, while the number of generations in medium stress is listed below each figure panel. Results for other stress ratios are similar. Note that trimodal distributions are never evolved for any stress conditions.

References

[1] Thattai M, van Oudenaarden A. Stochastic gene expression in fluctuating environments. Genetics. 2004 May;167(1):523–30.

[2] Visco P, Allen RJ, Majumdar SN, Evans MR. Switching and growth for microbial populations in catastrophic responsive environments. Biophysical Journal. 2010 Apr;98(7):1099–108.

[3] Rosenfeld N, Young JW, Alon U, Swain PS, Elowitz MB. Gene regulation at the single-cell level. Science. 2005 Mar;307(5717):1962–5.

[4] Charlebois DA, Kærn M. What all the noise is about: the physical basis of cellular individuality. Canadian Journal of Physics. 2012;923:919–923.

[5] Reshes G, Vanounou S, Fishov I, Feingold M. Timing the start of division in E. coli: a single-cell study. Physical Biology. 2008;5(4):046001.